UNIVERSITY OF OKLAHOMA

GRADUATE COLLEGE

EXPERIMENTAL INVESTIGATION OF HIGH TEMPERATURE EFFECT ON LOST
CIRCULATION MATERIALS FOR GEOTHERMAL APPLICATIONS

A THESIS

SUBMITTED TO THE GRADUATE FACULTY

In partial fulfillment of the requirements for the

Degree of

MASTER OF SCIENCE

By

CESAR VIVAS
Norman, Oklahoma

2021

EXPERIMENTAL INVESTIGATION OF HIGH TEMPERATURE EFFECT ON LOST
CIRCULATION MATERIALS FOR GEOTHERMAL APPLICATIONS

A THESIS APPROVED FOR THE

MEWBOURNE SCHOOL OF PETROLEUM AND GEOLOGICAL ENGINEERING

BY THE COMMITTEE CONSISTING OF

Dr. Saeed Salehi, Chair

Dr. Deepak Devegowda

Dr. Hamidreza Karami

Acknowledgments

I would also like to extend my thanks to my teammates and friends, Musaab, Nabe, Shawgi, Yuxing, Mustafa, Chinedum, Raj, Mjeed, Tobe, and Esteban; thank you for giving me your friendship, support, and motivation.

I wish to thank to Lina for being my best friend, partner, and wife, and my boys, Martin and Tomas. You are my greatest motivation, strength, and support. I love you deeply.

Thanks to my mom for being my guide in my journey to this life; I owe you everything.

Table of Contents

List of Figures

List of Tables

Abstract

Sustainable energy generation is crucial to meet the energy demands in the 21st century while keeping the implications of future challenges at its core philosophy. A geothermal power generation plant is one of such avenues that meet the associated challenges by utilizing the thermal energy stored in the earth to generate clean power. The energy acquired in the process, termed as geothermal energy, has the highest baseload due to its independence of seasonal factors (e.g., sunlight, winds, cloudiness). Despite the vast potential of geothermal energy, factors such as operational risks during drilling continue to limit its widespread development.

The geothermal drilling is impacted by a high-pressure and high-temperature (HPHT) environment at the subsurface. The high temperatures (HT) and the corrosive environment of geothermal drilling make the design of the drilling fluid a very complicated task. The HT geothermal drilling leads to major concerns, including thermal degradation. The drilling fluid thermal degradation impacts drilling processes such as the cuttings evacuation, hole cleaning, filtration, and fluid loss performance. These issues can lead to major operational problems such as massive mud losses, stuck pipe events, or poor cementing jobs if not adequately addressed.

Additionally, geothermal fields are characterized by the presence of highly fractured rocks. The combination of corrosive environment and fractured rock generates the need to incorporate additives for alkalinity, fluid loss control, and lost circulation. Research to analyze the effect of the additive's thermal degradation on the drilling fluid rheological properties in temperatures near or above 300°F (149°C) is limited. Thus, an extensive laboratory study is performed on water-based mud (WBM) drilling fluids.

Laboratory tests were performed using an HPHT rheometer to measure drilling fluid properties up to 400°F (204.5°C). Rheological properties, density, filtration, lost circulation, and alkalinity control additives at HT were measured during this work. Three different alkalinity control materials (Caustic Soda, Potassium Hydroxide (KOH), and Lime) were evaluated. Lime presented the best thermal stability at 400°F with an average variation of 2.4 cp (0.0024 pa.s) on apparent viscosity after three consecutive tests. Moreover, this alkalinity control material (lime) presented the least volume of mud gelled (2%) at HT. In contrast, Caustic Soda showed the highest volume of mud gelled (58%), adversely affecting mud rheology.

Additionally, twelve (12) different lost circulation materials (LCM) were tested for understanding their rheological behavior at HT. The study showed that HT has less impact on fine granular materials rheological behavior with an average increase of 17.7% compared with the baseline. In contrast, flaky, fibrous, and coarse granular materials presented an undesirable increase in rheology. The average rheology of the latter was 166% compared with the baseline.

The second stage of the experimental study consisted of performing laboratory investigation of LCM at HT. Eleven (11) different materials were tested; Walnut Fine, Walnut Medium, Sawdust, Altavert, Graphite Blend, Bentonite Chips, Micronized Cellulose (MICRO-C), Magma Fiber Fine, diatomaceous earth/amorphous silica powder (DEASP), Cotton Seed Hulls, and a Calcium Carbonate Blend. The filtration and sealing pressure of the LCMs were measured with HPHT equipment up to 300°F (149°C). Furthermore, the particle size distribution (PSD) of granular materials was measured. The results show that some LCM materials commonly used in geothermal operations are more sensitive to degrade at HT. Characteristics such as shape and size made some materials more prone to thermal degradation. Also, it was found that the PSD of LCMs is a key

factor in bridging and sealing fractures. The results suggest that granular materials with a wide particle size distribution PSD are more suitable for geothermal applications.

1. INTRODUCTION

1.1 Research Motivation and Research Hypothesis

The increase in energy demand worldwide has led to the rise in need for new energy generation sources such as renewable energy. Geothermal power generation is one of the most important renewable energy resources. A geothermal power generation plant benefits from the thermal energy stored in the earth to generate clean power. Geothermal energy is the renewable energy with the highest capacity factor. According to information from the U.S. Energy Information Administration (EIA 2020), the geothermal energy capacity factor averages 72% in the last ten years (Error! R eference source not found.). It is not uncommon for certain geothermal plants to reach values well over 90% (Sanyal and Enedy, 2011; Vivas et al., 2020). Because of its independence from seasonal factors, geothermal energy is one of the more efficient baseload power sources that can operate continuously to meet the minimum power demand 24/7.
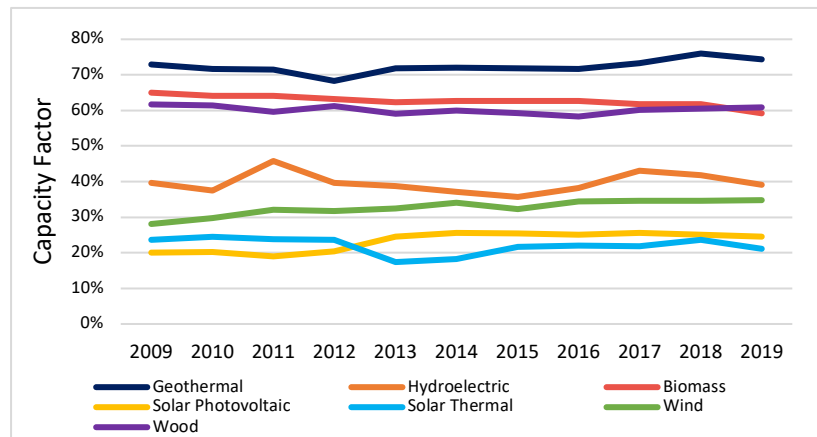
Figure 1.   Capacity Factors for Utility-Scale for Renewable Energy Sources 2009-2019 (Vivas et al. 2020)

Although its potential to provide constant energy, the widespread of geothermal production has been limited by various factors such as lack of access to thermal supplies, high capital costs, and operating

risks during geothermal well drilling. Marbun et al. (2013) described how operational problems associated with mud losses and stuck pipe events, causing the operational drilling times to be four times the amount of time initially planned in a field in Indonesia. Pálsson et al. (2014) described how non-controlled mud losses prevented the planned well depth from being reached in the Krafla field, Iceland. In this operation, multiple sidetracks were attempted, but the loss of circulation did not allow reaching the planned target. Bolton et al. (2009) described how total losses caused a well control event in the Wairakei field, New Zealand. To stop the blowout, a relief well to intercept the uncontrolled well was drilled. These examples depict how operational problems have a high impact on the drilling time scheduled, and therefore, the well costs.

The geothermal drilling process presents different challenges compared to conventional oil and gas drilling. A harsh environment with a combination of high temperature and hard rock makes the drilling process operationally complex. Special attention needs to be given to drilling fluids design and selection since it is the component of the well construction that is greatly affected by temperature changes. This component participates in every operation inside the drilling process. The most impactful problem during drilling geothermal wells is the mud losses. This is mainly due to the high frequency and the associated cost of loss of circulation events (Visser et al., 2018).

In typical geothermal wells, mud losses often correspond to a significant portion of non-productive time (NPT). Visser et al. (2018) reviewed the performance of geothermal wells in the United States. In **Figure 2**, a typical NPT distribution of wells with loss of circulation issues is shown. In that case, mud losses led to close to 200 hours of non-productive time. In the perspective of the rig rate, daily services, and mud lost in the formation, this particular case represented 24% of the well total cost (Visser et al., 2018). Cole et al. (2017) analyzed data from 38 geothermal wells drilled in the United States since 2009. The study found that wells accumulated more than 100 hours of non-productive

time on average due to loss of circulation, contributing to rig costs of an additional $185,000 or more per well. **Figure 3** shows the impact of mud losses on the average cost of a 50-MW geothermal plant. In this case, the loss of circulation represents 7% of the entire project, which shows how critical these events are in geothermal plant's capital costs.
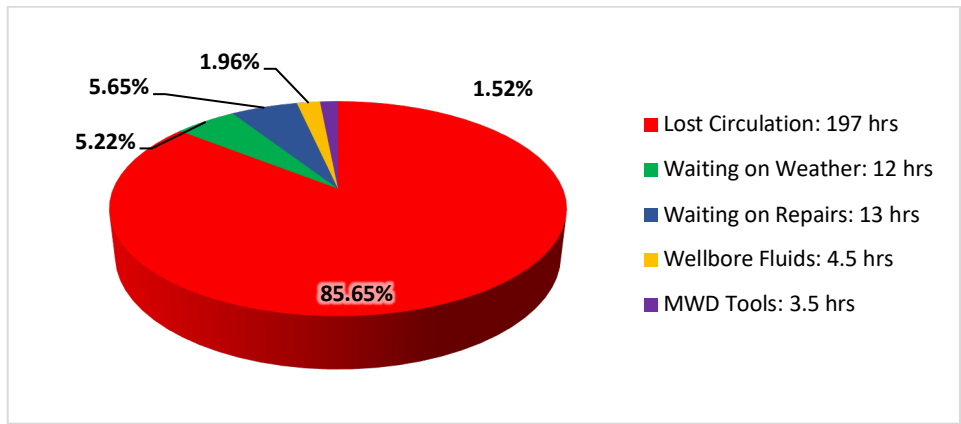
Figure 2. Non-productive time distribution in a well with mud losses (After Visser et al. 2018).
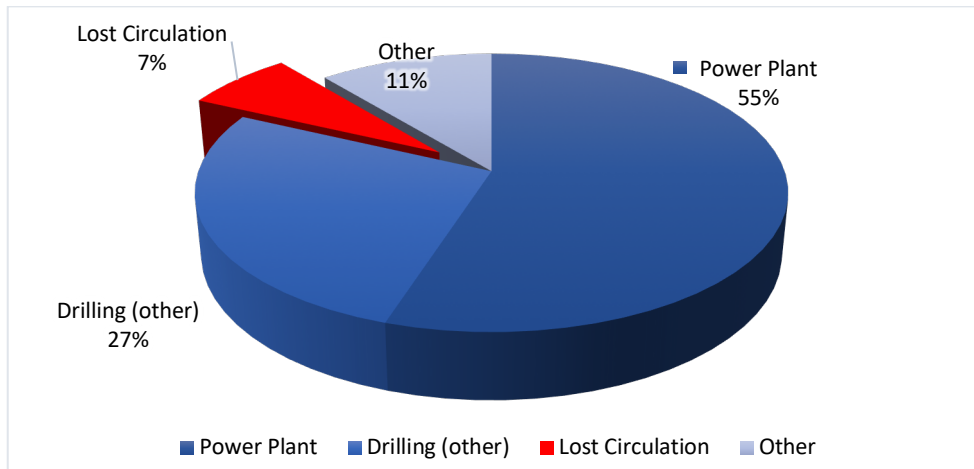
Figure 3. Capital cost decomposition for a typical geothermal 50-MW plant (modified from Cole et al. 2017).

Usage of lost circulation material (LCM) is necessary for intent to control mud losses. The incorporation of LCM in the fluid system affects the mud rheology. As drilling fluid rheology is also

affected by temperature increase, in geothermal operations, where temperatures reach close to and above 300°F, plastic viscosity and yield point are highly affected.

The most common detrimental effect of thermal degradation presented in geothermal operations is mud gelation. That can adversely increase the viscosity and generates an undesirable thicker filter cake. Even though all these problems are widely known, the rheology degradation of the drilling fluids exposed at HT is still not completely understood.

With the forgoing assessment of the drilling fluid effectiveness in geothermal drilling, the following hypotheses have been developed for this research:

1. The high-temperature encountered in geothermal drilling impacts the drilling fluid properties such as rheology.
2. The size and shape of the lost circulation materials significantly impact their effectiveness at high-temperature.

1.2   Research Objectives

The project's primary objective is to understand the effects of high temperature on the drilling fluid's properties to address the drilling fluid challenges present in geothermal drilling. To fulfill this goal, following secondary objectives are addressed:

1. Evaluate the temperature effect on different drilling fluid additives commonly used in geothermal applications.
2. Investigate the potential causes of mud gelation in high temperature, and provide possible solutions.
3. Provide a base mud recipe with thermal stability.
4. Characterize the impact of different lost circulation materials on drilling fluid rheology.

5. Perform a lost circulation materials screening for filtration and sealing pressure.

1.3   Research Outline and Scope of Study

In this study, different drilling fluid components were evaluated. Additives for viscosity, density, filtration, lost circulation, and alkalinity control were analyzed at HT. Three different alkalinity control additives and 12 different lost circulation materials were tested for understanding properties that made those components prone to fail at high temperatures. The experiments were conducted using an HPHT rheometer and an HPHT permeability plugging tester (PPT). This research is divided into the following sections:

1. Literature review: This section of the study provides a review of information related to geothermal drilling fluids, what are their characteristics, and the main challenges faced by the industry for addressing geothermal drilling fluids problems.

2. Experimental research: Laboratory tests were performed using HPHT equipment for measuring rheology and filtration. The focus is to understand the behavior of various WBM components and their properties at HT.

3. Post experimental analysis: The rheology and filtration tests are analyzed and contrasted with particle size distribution (PSD) analysis. PSD helped to understand some of the test results and support the main conclusions derived from this study.

2. LITERATURE REVIEW

This section presents how the industry has been addressing the thermal degradation in WBM based drilling fluids. Case studies in geothermal field operations were reviewed. Besides, studies related to rheological properties at HT are examined. Finally, an LCM review is presented.

2.1 Case Studies

The case studies presented are from operations in the US. Despite some of the information was generated in the '70s and '80s, problems depicted are still common today and not fully solved.

2.1.1 Imperial Valley

The Imperial Valley field is located in Southern California, and it is the second-largest geothermal field in the US. The Imperial Valley field's main sediments are sandstones, shales, claystones, and conglomerates deposited by the ancient Colorado River when it formed its delta (Cromling, 1973).

Fields in the Imperial Valley reach temperatures near to super-critical temperatures. Kaspereit et al. (2016) reported wells in the Salton Sea field with a bottom hole temperature of 390°C (734°F). The geothermal reservoirs in the Imperial Valley produces hot high-salinity brines, with pH values ranging from 5.7 to 7.6 (Liles et al., 1976). A freshwater gel-lignite mud was the drilling fluid widely found in the Imperial Valley. To initiate the well, a simple gel fluid was used. The increase in temperature led to mud gelation during operation. Lignite was used as a thinning agent to mitigate the adverse effects of mud gelation. The drilling fluid was then modified to a sodium surfactant fluid to finish the wells (**Table 1**).

Table 1.   Materials used to drill a well in Imperial Valley field (After Liles et al. 1976)

Material	Surface to 2,690 ft (lb)	2,690 ft to TD (lb)
Wyoming Bentonite	12800	-
Barium Sulfate.	16300	13,750
Treated Lignite	9750	-
Caustic Soda	1,700	2,500
Salt	-	1,700
Surfactant	-	4,600
Soda Ash	-	1900
Plastic Foil	-	650
Fine Walnut Hulls	-	2750
Fine Mica	-	4250
Cane Fiber	-	2,200

Zilch et al. (1991) identified three generations of drilling fluids for UNOCAL operations in the Imperial Valley field. The first generation started in 1976 with Sepiolite muds. These muds had good rheology but had insufficient fluid loss control and were prone to contamination by brine or cement. The mud contained Bentonite, Sepiolite, Caustic Soda, Lignite, and Sodium Salt. The second generation was a refinement of the first Sepiolite mud. The Bentonite and Lignite concentration in the system was increased. The Sepiolite was used mainly for viscosity building, and the Lignite was used to achieve filtration control. This second generation of drilling fluids had substantially increased filtration control efficiency relative to the initial generation. Such muds, however, had undesirable rheological properties and were highly prone to contamination. In the third generation of geothermal drilling fluids, the Sepiolite components were removed. The Wyoming bentonite was stabilized by a low molecular weight copolymer (sodium salt of maleic anhydride copolymer - SSMA-). The system also used Lignite and modified lignitic polymer compositions for better

filtration control. This fluid had rheological thermal stability, and the filtration properties were less affected by contaminants. **Figure 4** and **Table 2** presented each drilling fluid generation composition and a comparison of the effective viscosity measured by an HPHT rheometer.
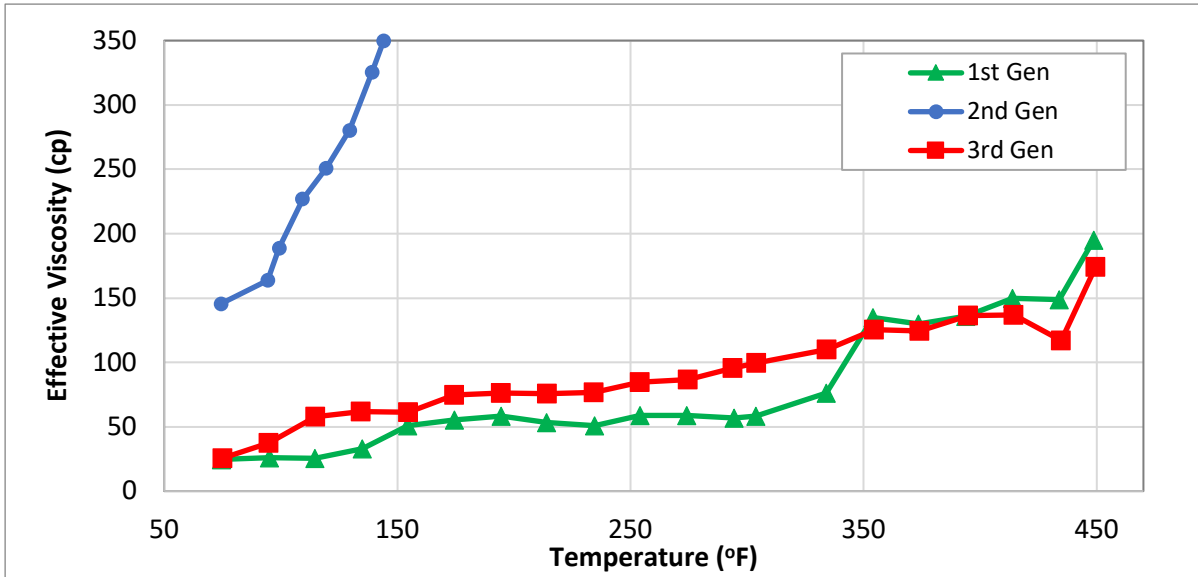
Figure 4. Comparison of effective viscosity at constant $100s^{-1}$ of the three generations of drilling fluids in Imperial Valley UNOCAL operations (generated with information from Zilch et al. 1991)

Table 2. Examples of the Drilling fluid composition of the three generations of drilling fluids in Imperial Valley UNOCAL operations (after Zilch et al., 1991)

	Additive	Concentration (ppb)
1ˢᵗ Generation	Bentonite	2.5
	Sepiolite	15
	Caustic Soda	0.2
	Sodium Polyacrylate	0.5
	Modified Lignite	1
	Drill Solids	20
2ⁿᵈ Generation	Bentonite	25
	Sepiolite	15
	Lignite	20
	Caustisized Lignite	10
	Caustic Soda	2
	Nonionic Detergent	5
	Drill Solids	20

3rd Generation	Bentonite	15
	HT Defloculant	0.75
	Modified Lignite	1
	Caustisized Lignite	1
	HT Polymeric Fluid Loss	0.75
	Drill Solids	20

2.1.2 The Geysers

The Geysers field is located in Sonoma County, Northern California. The drilling operations in this field started in 1955, and now it is the most extensive geothermal development in the world. Wells range from 3,950 ft to 9,000 ft, with reservoir temperatures from 450°F to 550°F (232.2°C to 287.8°C) (Grose, 1971). The production interval is mainly composed of sandstones (fine to medium-grained) with a minor proportion of shale, cherts, greenstones, and serpentines (Cromling, 1973). The Geysers is a dry steam geothermal resource (Finger and Blankenship, 2010).

The drilling fluid used in this field is a low-solid gel in freshwater containing lignin additives (Liles et al., 1976). Mechanical treatment using shakers, desanders, and desilters, was used to remove solids and combat increased viscosity to conserve a stable fluid. Aerated fluids are preferred when drilling in known loss circulation zones. This is to reduce the risk of formation damage associated with the clay particles in the water-based drilling fluid lost into the formation, which may seriously affect the reservoir's porosity and permeability.

Drilling fluids can also influence the cementing jobs. Firstly, they contaminate the cement. Secondly, drilling fluids that have been gelled and thickened leaves a thick filter cake in the formation and the casing, preventing the proper cement bonding. Besides, thickened mud can cause cement channeling behind the casing, leading to large zones poorly or not cemented. Such zones can

be filled with water that can vaporize at geothermal temperatures, creating voids that can lead to casing collapse (Varnado and Stoller, 1978).

2.1.3 Steamboat Springs

The Steamboat Springs field is located in southern Washoe County near Nevada's west border (White et al., 1964). The Steamboat field is a low-temperature field with bottom hole temperatures below 200°C (392°F) (Finger and Blankenship, 2010). Liles et al. (1976) described the drilling fluid used for drilling the Steamboat-1 well. The well was drilled with a low pH, Lignite-surfactant mud to a depth of 1,078 ft. A description of the materials used in the well is presented in **Table 3**.

Table 3.   Materials used in Steamboat 1 well (After Liles et al. (1976)

Material	Amount (Ib)
Wyoming bentonite	5,100
Barium Sulfate	34,900
Salt	100
Surfactant	1,640
Lignite	2,250
Soda Ash	400
Caustic soda	200
Diesel fuel	300-400

The objective of this formulation was to reduce/mitigate fluid losses and prevent cement contamination (Liles et al., 1976). The surfactant mud field trial showed that it was relatively easy and cost-effective to prepare and maintain. Test results indicated that the Lignite-surfactant fluid maintains acceptable filtration and rheological properties (**Table 4**).

Table 4.   Properties of Surfactant mud of Steamboat 1 well (after Liles et al. 1976)

Depth, ft	Weight, Ib/gal	Plastic viscosity, cp	Yield point, lb/100 ft3	Initial gel, lb/100 ft3	10 -min gel, lb/100 ft3	API filtrate, ml	Filter cake, in
393	10.3	30	8	4	9	3.6	2/32
432	10.6	28	12	2	10	4.2	2/32

462	10.7	29	10	4	9	3.6	2/32
523	10.8	30	7	4	9	3.6	2/32
603	11.1	34	6	5	9	3.6	2/32
634	11.4	36	7	4	6	3	2/32
873	10.7	19	3	3	6	3.6	2/32
1,030	11.4	42	12	3	7	3.6	2/32
1,077	11.1	47	12	3	17	3.8	2/32

2.1.4 Fenton Hills

Fenton Hills was the first hot-dry rock (HDR) project located in the Jemez Mountains, Northern New Mexico. The reservoir has temperatures from 195°C (383°F) to 235°C (455°F) (Brown, 2009). The drilling operation started in the late '70s. After numerous researches were conducted to evaluate HDR geothermal projects' concept in the '80s and '90s, the field has been temporally abandoned. Nuckols et al. (1981) described the challenges of the drilling fluids in Fenton Hills operations. The sedimentary portion of the wells (from the surface to 2,400 ft approximately) is compounded by volcanic and volcanoclastic sediments (Cenozoic rocks) in the upper section, and the lower section consists of massive limestones and shales (Paleozoic strata – Abo, Madera, and Sandia Formations). The drilling fluid used in that section was a polymeric flocculated bentonite mud. Red clay stringers in Abo Formation induced a significant increase in the drilling fluid viscosity (usually a funnel viscosity increase of 40 to 60 points) when hydrated. The most affordable approach applied for managing viscosity and mud weight was water dilution. Severe loss of circulation in the Sandia limestones caverns caused a reduction of the hydrostatic column, leading to the sloughing of the Abo and some of the Madera Formation beds. The consequences were stuck pipe events, repeated reaming, poor cement job, and intermediate casing damage.

Below the sedimentary formations are igneous and metamorphic rocks of Precambrian age (from 2,400 ft to 15,000 ft). This section well was drilled with water as the primary fluid. Very high

11

temperatures (608°F/320°C) and the abrasiveness of Precambrian Crystalline rocks caused corrosion problems. Due to these conditions, corrosion inhibition while drilling with clear water was complicated, considering the massive amount of water to provide sufficient cooling. Large quantities of an oxygen scavenger (ammonium bisulfite) and keeping a high pH in the system (9.5-11) successfully controlled corrosion (Nuckols et al., 1981).

2.2 Geothermal Drilling Fluids Properties

In principle, the geothermal drilling fluids have the same functions as O&G drilling fluids. However, the geothermal temperatures compromise some of their properties in terms of thermal degradation and corrosion.

Drilling reports from various geothermal wells in many reservoirs revealed common drilling mud properties (Finger and Blankenship, 2010). These properties are summarized in **Table 5**:

Table 5. **Typical Geothermal Drilling Fluid Properties (Information from Finger and Blankenship, 2010)**

Property	Range (SI Unit)	Field Units
Density	1.03 – 1.15 g/cm^3	8.58 – 9.58 ppg
Funnel viscosity	35 – 55 sec	35 – 55 sec
pH	9.5 – 11.5	9.5 – 11.5
Plastic viscosity	0.01 – 0.02 Pa-s	10 – 10 cp
Yield point	35 – 125 kPa	7.3 – 26.1 lbf/100ft^2

2.2.1 Density

Mud density is one of the most common properties of drilling fluid and must be accounted for during well planning. Mud density must be designed considering the pore pressure (formation pressure) and the fracture gradient expected. In geothermal applications, it is not rare that formation pressures

are lower than O&G wells. WBMs of 9 to 10 ppg are typically used for geothermal drilling, though aerated muds are used to prevent mud losses (Liles et al., 1976). A geomechanical study is essential to understand the near-wellbore stresses to avoid or limit wellbore instability (breakouts).

Usage of weighting agents in geothermal drilling is rare since minimum mud densities are desired to minimize lost circulation problems.

Density can be raised using weight additives such as Barite (the most common weighting agent) without unnecessarily modifying other drilling fluid properties. Density incremented by drilling solids (e.g., cuttings, cavings, sand, silt, among others) is undesirable. Adverse effects derived from the rise of drilling fluid density using solids include reducing the rate of penetration (ROP), filter cake thickening, and the wear of BHA/drill pipe tubular and mud pump parts by abrasion (Culver, 1998).

2.2.2   Viscosity

Viscosity in a drilling fluid property that must be monitored when working in a high-temperature environment. Viscosity is highly affected by temperature changes. Thermal degradation of drilling fluids can be manifested in terms of reduction in plastic viscosity (PV) and yield point (YP). This affects the drilling cuttings carrying capacity and then the hole cleaning. Besides, thermal degradation can cause mud gelation. The latter causes an uncontrolled increase of viscosity, leading to stuck pipe events or debonding during cementing jobs.

The effect of HT in WBM was studied by Amani and Al-Jubouri (2012). In that study, different drilling fluids were tested at HPHT conditions. The drilling fluids were tested at temperatures from 100°F to 500°F (37.8°C to 260°C) and confined pressures from 5,000 to 35,000 psi. The authors found the temperature increase impacted rheological properties regardless of the testing pressure

(**Figure 5 right**). In contrast, the pressure increase has a lesser effect on plastic viscosity (**Figure 5 left**).
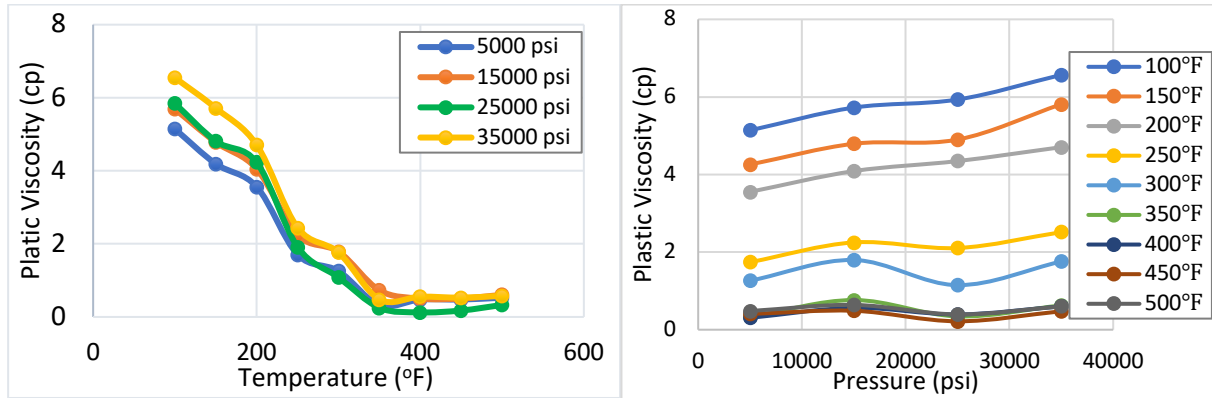
Figure 5.　　Plastic Viscosity Versus Temperature [Left] and Plastic Viscosity Versus Pressure [Right], (After Amani and Al-Jubouri, 2012).

From the same research, the yield point (YP) was found to behave similarly. The authors of the study suggested that the behavior of rheological properties of the drilling fluids tested under HT is the product of the thermal degradation of the mud components. The resultant molecular expansion of the mud components lowers the resistance of the drilling fluid to flow, and thus, its PV, YP, and gel strength.

Similar effects were observed by Galindo et al. (2015) in laboratory tests of a high-performance WBM at HPHT condition. Rheology values at different temperatures are shown in **Table 6**, where it can be observed how PV and YP reduce with temperature.

Table 6.　　Rheology of 14 ppg HT/HP WBM formulation from 120 to 400 °F (After Galindo et al., 2015).

Temperature (°F)	120	120	250	300	350	400
Pressure (psi)	0	2000	2000	2000	2000	2000
PV (cp)	34.0	29.3	17.6	14.2	13.2	12.7
Yield Point (lbf/100ft2)	26.0	38.4	18.4	13.2	10.5	10.4
600 rev/min	94.0	97.0	53.6	41.6	36.9	35.8
300 rev/min	60.0	67.7	36.0	27.4	23.7	23.1

14

200 rev/min	48.0	54.8	29.5	23.4	20.1	20.2
100 rev/min	33.0	39.2	21.8	17.6	15.7	15.9
6 rev/min	12.0	15.9	9.1	7.8	7.0	7.6
3 rev/min	10.0	14.4	7.9	6.9	6.1	6.8

The most common effect of the HT observed in geothermal wells is the mud gelation (Cromling, 1973; Finger and Blankenship, 2010; Liles et al., 1976; Tuttle, 2005; Tuttle and Listi, 2003; and Varnado and Stoller, 1978). Tuttle and Listi (2003) suggested that gelation is caused by the solids drilled contending strongly for the free water in the fluid system, contributing to mud dehydration and a severe rise in viscosity. This unfavorable condition increases the frictional pressure losses during circulation, leading to an increase in the equivalent circulation density (ECD). This condition in narrow mud window operations could lead to induce mud losses. Other adverse effects of mud gelation are stuck pipe events or poor debonding during cementing jobs.

Viscosity, according to the needs, can be increased using viscosifiers or decreased using thinning agents. API quality Bentonite is the predominant viscosifier for geothermal drilling. Required rheological properties can be controlled with Bentonite in moderate concentrations (5-20 ppb), with proper filter cake and viscosity results (Tuttle, 2005). Nevertheless, not all Bentonites are recommended for geothermal operations. Sepiolite and Attapulgite can generate adverse effects such as wellbore instability, thicker filter cake, and inadequate PV and YP. The usage of high-quality Bentonite clay is recommended (Tuttle and Listi, 2003).

Polymer application in the mud system is practical; however, it is affected when exposed to HT for a long time (Finger and Blankenship, 2010). Their primary application is for high viscosity pills to ensure hole cleaning before wiper trips, electric logs, running casing/liners, or cementing jobs. Besides, it is essential to reduce the viscosity when HT gelation or the solids content in the drilling

fluid is undesirably high. Recent advances in HPHT polymers have shown success in provided mud thinning and gel inhibition (Finger and Blankenship, 2010).

2.2.3 Alkalinity

Selecting the appropriate fluid alkalinity is essential for the control of corrosion during geothermal drilling. Geothermal drilling fluids with high pH are essential to regulate the effects of certain wellbore pollutants (CO_2 and H_2S). This is indispensable in mitigating corrosion and improving certain drilling fluid additives (Finger and Blankenship, 2010). Caustic Soda has been added for alkalinity control in fields such as The Geysers, Imperial Valley, and Steamboat Springs (Liles et al., 1976). The incorporation of caustic soda in the system has been a conventional way of increasing alkalinity. However, Caustic Potash (KOH) is increasing its popularity in geothermal applications due to its advantages in wellbore stability (Tuttle, 2005).

2.2.4 Filtration

This property represents how well the drilling fluid builds an impermeable coating on the wellbore wall to avoid leakage into the permeable rocks. The hydrostatic pressure of the drilling fluid column must be higher than the pore pressure. The objective is to prevent the influx of the formation fluids. The filter cake can prevent the drilling fluids from penetrating the permeable formations. It is necessary that the mud quickly generates a filter cake capable of reducing fluid loss. Besides, filter cake needs to be sufficiently thin and easy to remove to permit the production flow into the wellbore throughout the production stage of the well (Caenn et al., 2016).

Various additives for filtration control apply to geothermal drilling operations. The most commonly used is Lignite, thanks to its low cost and high accessibility. Lignite concentrations up to 12-20 ppb are also needed for sufficient filtration control. However, thermal degradation can potentially

16

generate carbonate contamination in the mud, contributing to an inadequate, very high viscosity (Tuttle and Listi, 2003).

2.3   Drilling Fluids Components and Formulation

In general, drilling fluid systems consist of base fluid (in WBM drilling fluid, the base fluid is water), active and inert solids, and additives to preserve the mud properties. These components control the main drilling fluid properties; density (e.g., mud density, specific gravity), viscosity (e.g., PV, YP), and chemical reactivity. In geothermal drilling fluids, the most relevant properties are alkalinity, formation stability and inhibition, filtration, and fluid loss control.

As a minimum, a drilling fluid formulation designed to address geothermal drilling challenges must include a stable thermal viscosifier, a filtrate control additive, a pH buffer, and LCM if mud losses are expected. In addition to the high-temperature constraints, the main limitations are the low-density requirement and the additives' cost. Some high-tech HPHT additives are cost-prohibited for geothermal applications, which could easily turn a technically properly designed well into an economic failure (Vivas et al., 2020).

Tuttle (2005) presented a summary of different additives recommended for geothermal applications based on field experience or promising lab tests (**Table 7**). To generate a basic formulation that meets the conditions mentioned above, the additives presented in the cited table provides an initial step since some of the components can be easily found.

Table 7.   Product Selection Criteria for Geothermal Drilling Fluid (After Tuttle, 2005).

Property/Characteristic	<350°F (<177°C)	>350°F (>177°C)
Rheology Control (Viscosity Increase)	API Bentonite, Synthetic Polymers	API Bentonite, Synthetic Co-Polymers

Rheology Control (Thinning)	Polyacrylates, Desco CF	New Co-Polymer Blends, Lignite, Desco CF
Filtrate/Water Loss Control	PACs, Starch Derivatives, Acrylamides	HT PAC Blends, Modified Acrylamides, Lignite
Alkalinity/pH Control	Caustic Soda, KOH, Lime	Caustic Soda, KOH, Lime
Inhibition/Lubricity	K+, Al+++-Based Additives, Gilsonite, TORKease	K+, Al+++-Based Additives, Gilsonite, TORKease
Lost Circulation	Cottonseed Hulls, Sawdust, Crosslink Plugs	Cottonseed Hulls, Sawdust, Crosslink Plugs

2.4 Mud Losses in Geothermal Drilling

Lost circulation is caused by mud entering into porous or fractured rock, causing the reduction in the hydrostatic column (mud column). In this case, the mud is getting into the formation instead of returning to the surface (Hinkebein et al., 1983). The mud loss is the most severe problem during the drilling of geothermal wells, mainly due to its high frequency and associated high costs. In geothermal reservoirs is common to find complex fractures networks (Rossi et al., 2020). This highly fractured rock environment is one of the most common causes of massive mud loss events. Fractures that measure 1 to 3 thousand microns or more are complicated to cure at high temperatures (**Figure 6**). Even though this is an extensively studied phenomenon, lost circulation is still the most problematic and costly issue in geothermal drilling (Vivas et al., 2020).

Figure 6.   **Large fracture in a geothermal well core sample (Blankenship, 2016)**

Goodman (1981) conducted a study of how the geothermal industry addressed mud losses during drilling operations. After an extensive survey, Goodman observed that geothermal operators used traditional O&G drilling approaches to solve drilling fluid losses (LCM's, pills, or cement plugs). The study revealed that, depending on the individual downhole conditions, these approaches may or may not be effective in resolving impaired circulation. Hyodo et al. (2000) analyzed close to 4,500 lost circulation events in Japan. In that study, 65% of the wells presented total losses, and when those losses were treated with LCM', the success rate was about 10%. At present, despite the evolution of LCM materials, the treatment's success rate is still low. Cole et al. (2017) analyzed the mud losses in 15 wells in California. The effectiveness of lost circulation materials in both; LCM incorporated into the fluids system (**Figure 7**) and LCM pills spotted downhole (**Figure 8**) were evaluated. The analysis was divided into seepage losses (less than 25 bbl/h), partial losses (among 25 to 100 bbl/h), severe losses (greater than 100 bbl/h with drilling fluid returns), and total losses (no returns of drilling fluid). Ninety-five events in total were analyzed, and the overall success rate of all treatments with LCM was 25.3%. In general, it can be observed that partial and severe losses, the treatments have a better success rate, compared with their performance at total losses, where all

LCM treatments failed. Total losses in geothermal wells are commonly attributed to fractures that are difficultly healed with LCM.
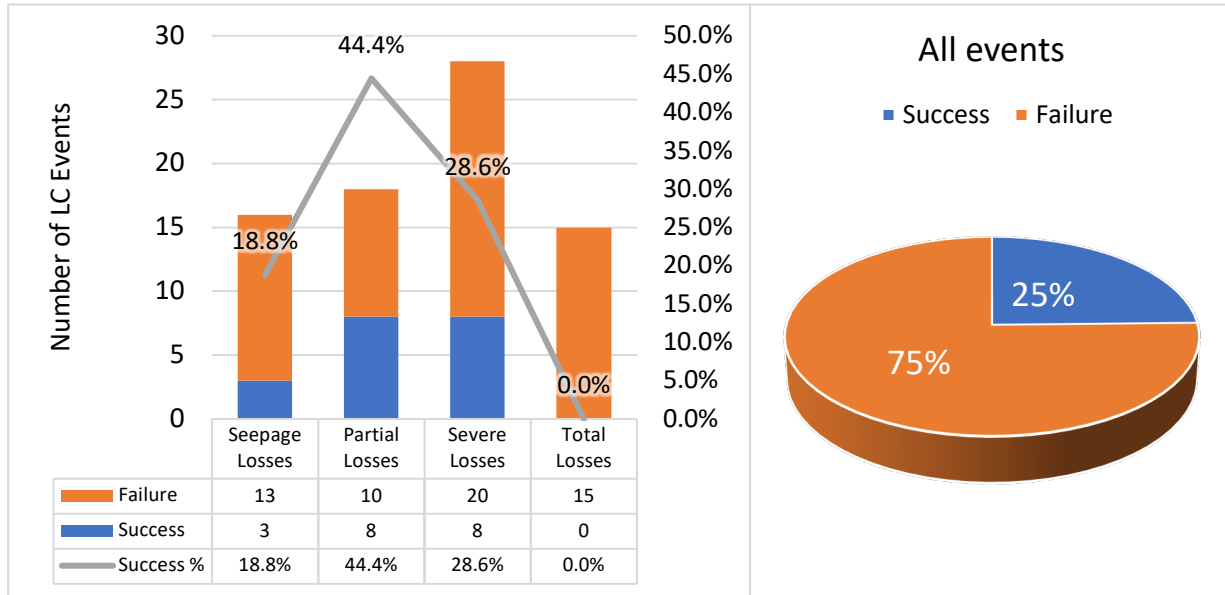
Figure 7. The success rate of losses remediation with LCM materials incorporated into the fluid system plot generated with information from Cole et al., 2017).

In the same study, the effect of temperature and depth was analyzed. In **Figure 9,** LCM treatments are showed by depth and formation temperature. The temperature range of data analyzed is mostly among 150°F (65.6°C) and 300°F (149°C). Some LCM's and drilling fluids started to degrade at temperatures above 250°F (121.1°C). However, there is no indication that temperature increase has a remarkable effect on the losses remediation success/failure ratio in the information presented. Failure of losses curing also happens at temperatures way below 200°F. Failure in sealing can probably be attributed to an LCM selection rather than thermal degradation in the wells analyzed. Paper, cottonseed hulls, nutshells, and calcium carbonate were used in 87% of all events. According to interviews with drilling operators of the wells, the LCM components were mostly selected on a well-by-well basis through trial and error rather than formation properties. The severity of losses provided to operators an indication of whether materials should perform well based on previous experiences.
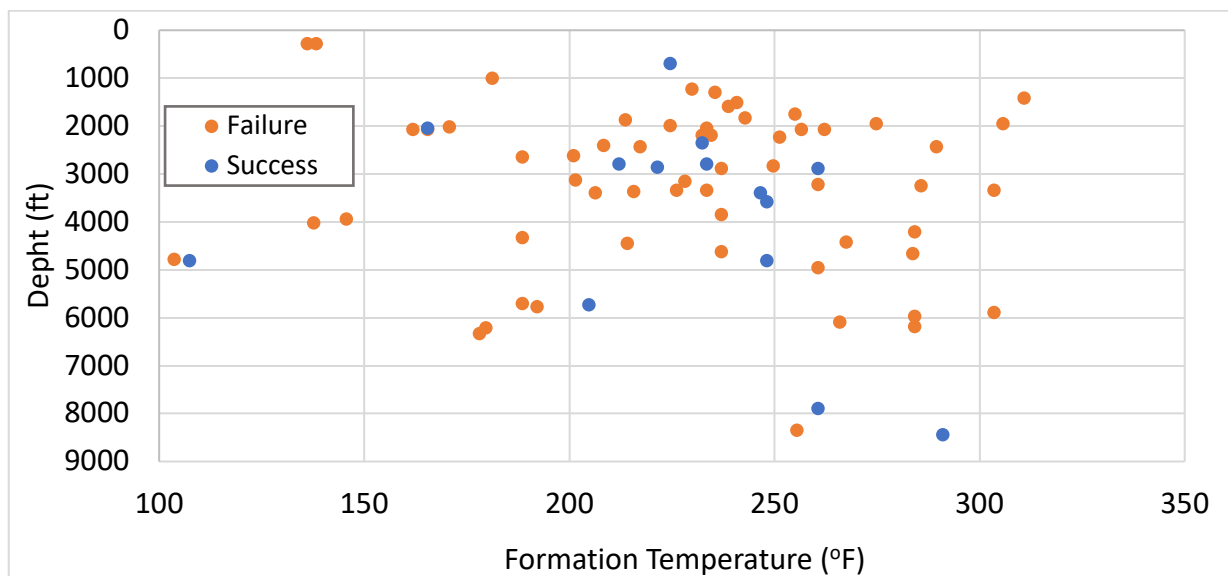
Figure 9.   **LCM treatments effectiveness from temperature vs. depth perspective (plot generated with Cole et al., 2017).**

2.4.1 Addressing Mud Losses - History Cases

Liles et al. (1976) and Zilch et al. (1991) reported that drilling fluids in Imperial Valley used Lignite or modified lignitic polymer compositions for filtration control. Liles et al. (1976) reported that lost circulation zones are present anywhere along the wellbore. Circulation of LCM was necessary to restore mud returns. However, sometimes the rock in the lost circulation zone collapses to heal the mud losses itself. In the same report, a lost circulation event on the East Mesa lease was described. Total losses were presented at 7,419 feet, and circulation could not be recovered by circulating various LCM's (fiber, cottonseed hulls, or mica flakes, among others). Finally, a cement job was necessary to cure losses.

Cromling (1973) reported that mud losses are typical in the Geysers due to the highly fractured zones. In the same study, cottonseed hulls were reported to be the most commonly used LCM, and 12 ppb was a typical concentration to address mud losses in the field. Occasionally, when mud circulation could not be restored, cement was used to cure mud losses.

Nuckols et al. (1981) described a severe loss of circulation case in Fenton Hills (Jemez Mountains, Northern New Mexico). Several attempts to cure losses were performed, including the circulation of bridging agents (1500 bbl of LCM at 30% of volume), and cementing jobs were performed without success. Finally, it was decided to drill without returns and run the casing to isolate the loss sections. The consequences of mud losses were stuck pipe events, repeated reaming, poor cement jobs, and intermediate casing impairment.

Geothermal formations are commonly under-pressured, with differential pressure (the difference between the hydrostatic pressure of the drilling fluid column and the formation-pore pressure) usually above 500 psi. If the surge pressure when drill pipe is tripping downhole is added, which is

commonly around 500 psi, that gives a total value of 1,000 psi of sealing pressure (or differential pressure), which is used as a reference value for geothermal applications (Hinkebein et al., 1983).

Functional consequences of lost circulation are diverse, but the most critical are stuck pipe, well-control, and casing-cement issues (Vivas et al., 2020).

2.4.2 Lost Circulation Materials

In general, geothermal drilling operators have available LCM's at the rig site for immediate usage once mud losses are present. The materials are incorporated into the mud system and circulated downhole to control the losses, making LCM the first defense line operators prefer (Hinkebein et al., 1983).

Caenn et al. (2016) divided lost circulation materials into four categories summarized in **Table 8**.

Table 8. **Lost Circulation Materials Classification**

LCM Type	Examples	Characteristics
Fibrous materials	Sawdust, cedar fiber, shredded cane stalks, cellulose, bagasse, cotton fibers, shredded automobile tires, wood fibers, paper pulp	• Flexible materials • Variable sizes • Tend to be squeezed into wide openings
Flaky materials	Wood chips, shredded cellophane, mica flakes, plastic laminate	• Flat shape • Large surface area • Can be squeezed into openings
Granular materials	Calcium carbonate, ground nutshells, granular marble, Formica, corncobs, cotton hulls, granular graphite, micronized cellulose	• Chunky granular shape, with a variety of grain sizes. • Strong and stiff materials • Ideal materials are insoluble and inert inside the mud.

Slurries	Hydraulic cement, diesel oil-bentonite-mud mixes, and high filter loss muds	• Designed to harden with time

As observed, LCM's are diverse in shape, density, or stiffness, and depending on their attributions, they work differently in reducing and avoiding drilling fluid get into the formation.

Another group of LCM material is the engineered polymers. The usage of polymers for addressing mud losses in geothermal drilling has been investigated. Magzoub et al. (2020) presented different applications of crosslinked polymers as LCM in HPHT applications. Mansour et al. (2019) introduced a shape memory polymer that can be programmed to expand at a predetermined temperature. Polymers and silicates can be used for plugging fractures at 350°C (575°F) or above for an extended time (Bauer et al., 2005, 2004; Mansure et al., 2004). Micronized Cellulose has been applied successfully in geothermal operations in low-density drilling fluids (8.5 to 8.9 ppg) as individual LCM (Rickard et al., 2012; Samuel et al., 2011).

2.4.3 Previous LCM Experimental Research at HT

Experimental research had been performed to evaluate the performance of LCMs. Although some experimental studies have been performed at room temperatures, they had been fundamental to understanding the sealing mechanisms. Others have tried to evaluate the performance of temperature-aged LCMs to understand their impact under geothermal conditions, but the tests are performed at room conditions. Few experimental studies have been conducted measuring properties directly at high temperatures. This is due to the challenges of managing temperatures of 300°F (149°C) and above. High pressures (necessary to avoid evaporation), very long heating and cooling times, or testing equipment wear (especially elastomers) are some of HPHT research limitations.

Howard and Scott Jr. (1951) made an experimental study of different LCM performance at dynamic conditions and room temperature. They measured the sealing capability (a seal capable of holding 1,000 psi of differential pressure) using different fracture sizes versus material concentration (**Figure 10**). One of the experimental study outcomes is that granular materials are more effective for closing large fractures (up to 5,000μm). Researchers found that granular LCM requires less material concentration to seal similar size fractures compared with fibrous and flaky LCMs.
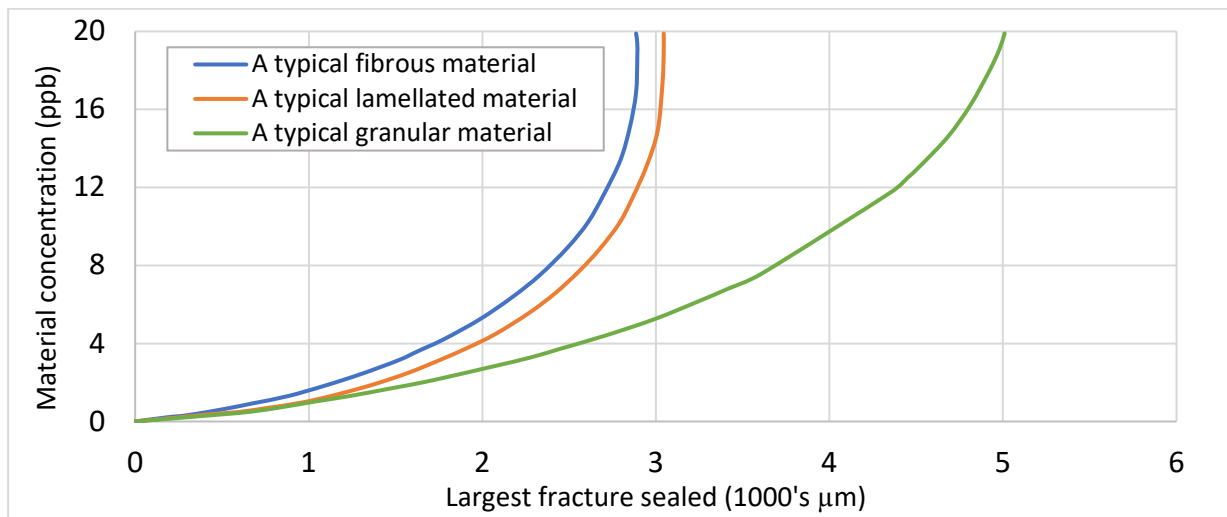
Figure 10.   Effect of LCM concentration at different fracture sizes (After Howard and Scott Jr., 1951)

Hinkebein et al. (1983), in another experimental study, three cellulosic materials were studied: cottonseed hulls, Kwik-Seal (a combination of granular, fibrous, and flakes components), and Ruf-Plug (ground corn cobs). Paper pulp was also tested, but due to poor results, it was dropped from the study. All materials were tested with a low-density drilling fluid (8.8 ppg), compounded by water and Wyoming bentonite. According to the results presented, derived from extensive laboratory experiments (223 experiments), the LCM concentration increase in all three materials increases the likelihood of successful sealing (**Table 9**). However, they found that the LCM concentration increase for the materials tested does not conclusively increase the sealing pressure. The conclusion

was due to the results' randomness, where the same type of material was tested under the same conditions, and sealing pressures cannot be replicated.

Table 9. **Comparison of Percentage of Successful 1000 psi Sealing Pressures at Different Concentrations**

Slot Size	Cotton Seed Hulls			Kwik-Seal			Ruf-Plug		
in	5 ppb	10 ppb	Dif	5 ppb	10 ppb	Dif	5 ppb	10 ppb	Dif
0.06	66.7%	100.0%	33.3%	100.0%	100.0%	0.0%	66.7%	100.0%	33.3%
0.08	37.5%	100.0%	62.5%	33.3%	100.0%	66.7%	0.0%	11.8%	11.8%
0.12	6.7%	20.0%	13.3%	11.8%	45.5%	33.7%	0.0%	0.0%	0.0%
0.16	0.0%	0.0%	0.0%	0.0%	54.5%	54.5%	-	0.0%	-
0.2	0.0%	7.7%	7.7%	0.0%	23.1%	23.1%	-	0.0%	-

In the same research, the temperature effect was analyzed. In this case, the materials were hot rolling aged at different temperatures (**Figure 11**). The results show that all materials at room temperature managed to seal the 0.06" (1524μm) fractures, reaching 1000 psi of sealing pressure. However, when materials were tested after being hot-rolling at 400°F (204.5°C), cottonseed hulls and Ruf-Plug LCM failed to seal the fracture, and the Kwik-Seal lost 30% of its sealing pressure strength. These results suggest that thermal degradation of LCM's properties affect their sealing performance.
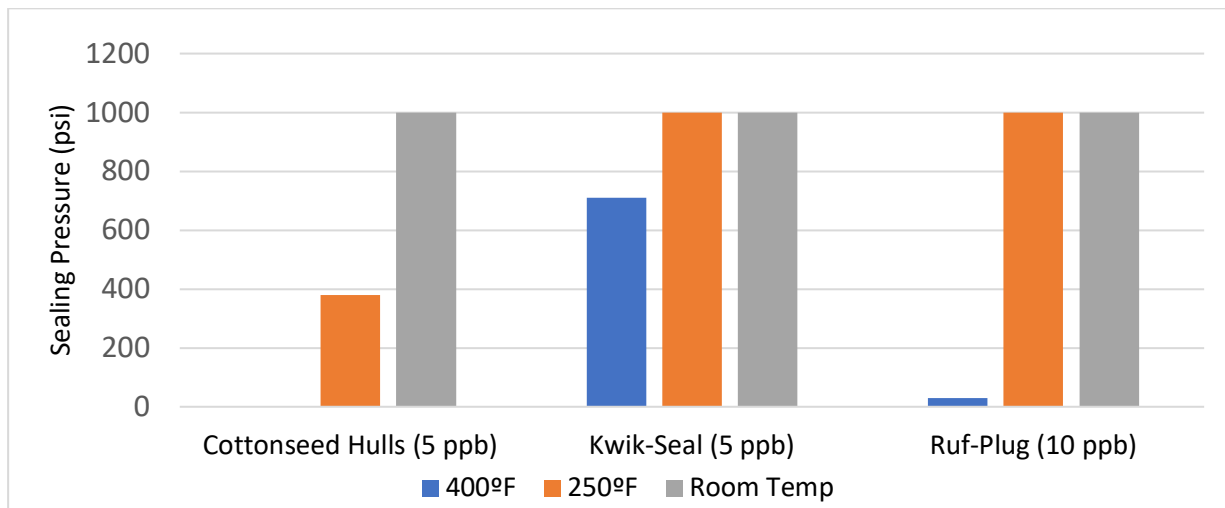
Figure 11. **Sealing pressures of three cellulosic LCM products at different temperatures using a 0.06" (1524µm) fracture (plot generated with information from Hinkebein et al., 1983)**

2.4.4 Bridging and Sealing

The process in which LCM is utilized to cure mud losses has been analyzed for years. LCM creates a restriction that avoids or at least reduces fluid loss by plugging the pores and fractures in the borehole. The addition of LCM to the drilling fluid increases the particle size distribution to plug pores or fractures (White, 1956). However, frequently, LCM usage in geothermal drilling is based on trial and error or based on experience rather than as a product of an optimization analysis (Cole et al., 2017).

The life cycle of how LCM works can be divided into four stages; dispersion, bridging, sealing, and sustaining (Lavrov, 2016).

Dispersion is how the LCM arrives at the fracture. The LCM must overcome various restrictions during its journey through the mud pits and pumps system, the journey through the drill pipe, and the restrictions of the different components of the BHA until it reaches the fracture.

Bridging consists that once LCM gets into the fracture, they start forming a permeable layer across the fracture, robust enough to withstand the pressure gradients, and hold smaller particles that will create the seal.

Sealing is the process in which the small particles, either undersized LCMs or mud solids (p.e., bentonite, barite), accumulates on the bridge built by the coarse LCM. These smaller particles fill all the spaces of the bride, generating an impermeable layer. This layer prevents the fluid continue passing through the fracture.

27

Sustaining is fundamental since the seal generated by LCM needs to withstand mechanical loads and differential pressure enough time to permit drill through the theft zone, case, and cement the well.

Understanding the process is important for a successful sealing strategy. One of the most important factors is the size of the LCM. If the bridging material is larger than the fracture width, the sealing will be formed outside the fractures' mouth. This is undesirable since the drilling action can easily remove it. In contrast, if LCM is too small compared to the fracture size, it cannot effectively build a bridge (Lavrov, 2016). As fractures in geothermal wells can vary in size, and LCM strategy may consider diverse particle sizes. A particle size distribution analysis is essential. The sealing and bridging process is depicted in (**Figure 12**)
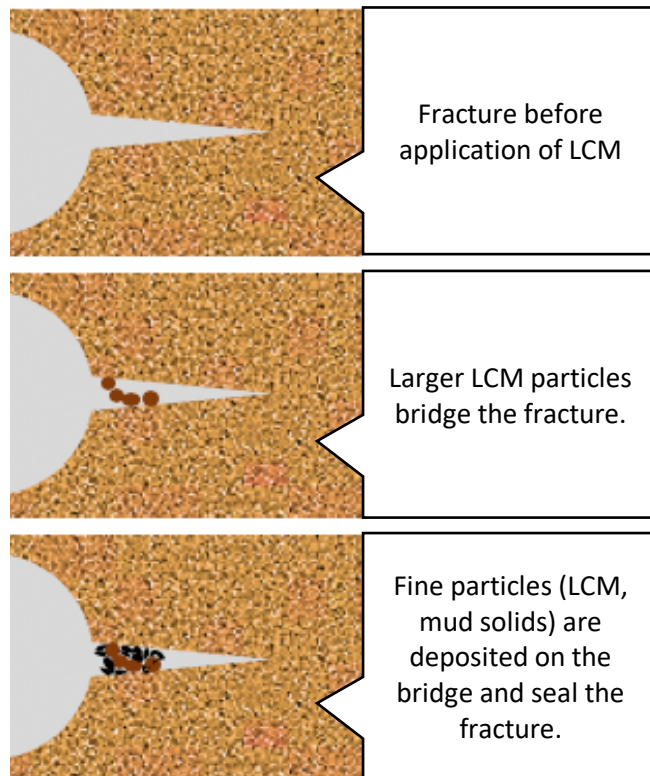
Figure 12.   **LCM bridging and sealing process (Adapted from Lavrov, 2016)**

The connection between the particle size of an LCM and its capability to bridge fractures has led to the development of different methods to select the proper particle size.

One of the most accepted criteria was proposed by Abrams (1977). The method is consisting of two rules for selecting bridging material. The first rule is that the particle size's mean size must be equal to or greater than one-third of the mean of the rock pore size. The second rule is that the sealing material must be no less than 5% of the drilling fluid volume.

Since then, different criteria have been proposed. They are summarized in **Table 10**. The downside of the earlier methods is that they are based on pore size. However, they have been used as selection criteria for sealing fractures. Alsaba et al. (2017) proposed a new selection criterion based on a statistical analysis of extensive experimental research. LCMs with diverse particle size distributions were tested on fractures from 1000 μm to 3000 μm.

Table 10.   **Summary of LCM selection by Particle Size (After Alsaba et al., 2017)**

Method	Selection Criteria	Authors
Abrams Rule	D50 ≥ 1/3 the formation average pore size	Abrams, 1977
D90 Rule	D90 = the formation pore size	Smith et al., 1996
		Hands Velsen et al., 1998
Vickers Method	D90 = largest pore throat	Vickers et al., 2006
	D75 < 2/3 the largest pore throat	
	D50 ≥ 1/3	
	D25 = 1/7 the mean pore throat	
	D10 > the smallest pore throat	
Halliburton Method	D50 = fracture width	Whitfill, 2008

Alsaba Method	D50 should be $\geq$ 3/10 the fracture width	Alsaba et al., 2017
	D90 should be $\geq$ 6/5 the fracture width	

2.4.5 Wellbore Strengthening

An evolution to the traditional LCM addition to the mud system is the concept of wellbore strengthening. This consists of LCM usage to intentionally increase the fracture gradient of a wellbore by adding LCM to bridge and seal fractures near-wellbore (Salehi and Nygaard, 2011). Three physical models describe the wellbore strengthening concept and how they enhance the wellbore strength in drilling operations; stress cage model, FCS (Fracture Closure Stress) model, and FPR (Fracture Propagation Resistance) model (Magzoub et al., 2020).

The concept of stress cage was introduced by Alberty and McLean (2004), and it explains how mud additives help to seal fractures induced during drilling. The stress caging theory is to place solids at or close the mouth of a recently drilling-induced fracture that will serve to build a bridge. The bridge creates the support to hold particles that generates the seal, insulating the drilling fluid pressure from the rest of the fracture. If the seal is successful, the fluid pressure of the isolated portion of the fracture will be dissipated to the pore pressure. Then, the fracture, without the pressure that maintains it open, will close (**Figure 13**). This process increases the hoop stress around the wellbore beyond its original value.

30
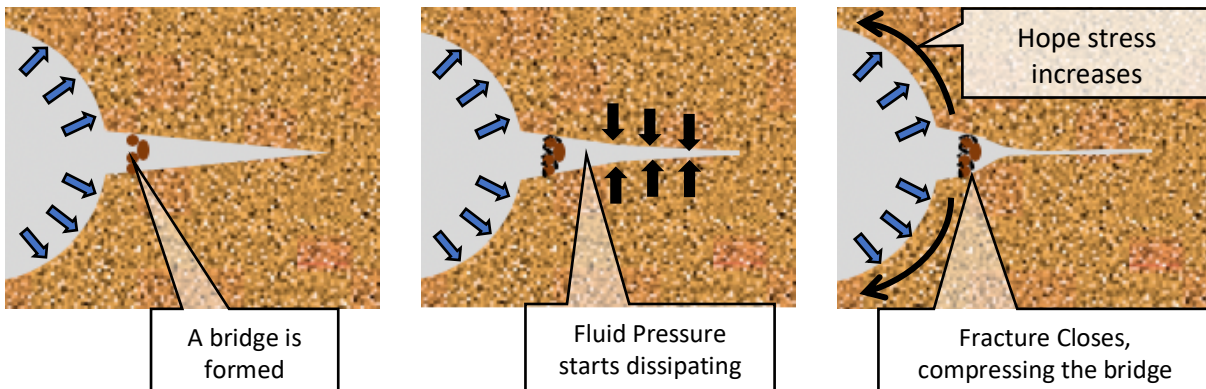
Figure 13.   Stress cage process (after Alberty and McLean, 2004)

In the FCS model (**Figure 14**), a fracture in the wellbore is generated and widened, expanded in length but not in width. LCM is forced to fill the fracture. LCM starts to accumulate inside the fracture, and as the carrier fluid is filtrating into the formation, it creates an "immobile mass" within the fracture. The immobile mass holds the fracture open and isolates the fracture end from the drilling fluid pressure. Fracture is getting more difficult to open due to increased fracture closing tension and the fracture end isolation (Dupriest, 2005).

Fracture widens until it will accept barite-sized particles, then it will increase its length but not its width

Fluid loss creates immobile mass. Fracture pressure increase as mas resist hydrostatic head. Pressure widens the fracture

Pressure is held. Filtrate loss continues until fracture is packed back to the wellbore. Width and increased FCS are trapped by solids.

In low permeability, or if great width is required, hesitation is conducted to build width in layers.

Figure 14.   Fracture Closure Stress process (based on Dupriest, 2005)

In the FPR model, unlike FCS and stress cage models, the hope stress is not increased (Magzoub et al., 2020). This wellbore strengthening approach relies in the continuous addition/maintenance of lost circulation materials. The concentration of the latter is supported by the continuous recovering

and re-usage of solids, that contributes to generate a fracture resistance propagation (Van Oort et al., 2011). The idea is that a mud cake generates an impermeable layer that prevents the drilling fluid pressure from expanding the fracture (**Figure 15**) (Morita et al., 1996).
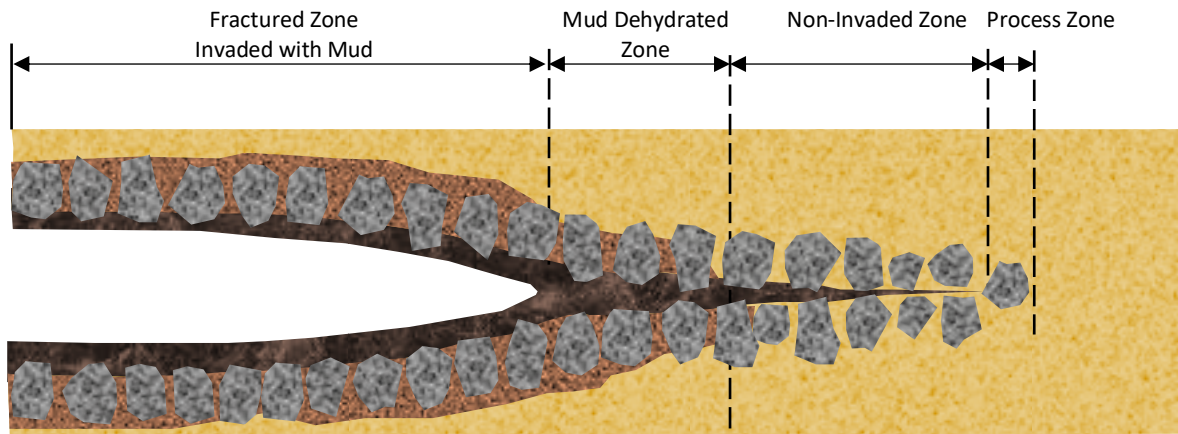
Figure 15. **Cross-section view of mud cake formed around a fracture tip (Based on Morita et al., 1996).**

2.4.6   Fracture Size Estimation

Fracture size estimation is one of the most challenging properties to be identified. Acoustic and electric image logs and conventional logs can be used to determine fracture size (Ran et al., 2014). Also, fracture size can be determined in the laboratory, measuring directly from core samples (Huy et al., 2010). The limitation of the mentioned methods is that they required well/s previously drilled.

Estimation of the fracture size in unexplored areas is more difficult. Without wells drilled, surface geophysical methods are the main tools to detect fractures. P-wave methods can provide fracture direction, azimuth, and fracture density (Rüger and Tsvankin, 1997). Elastic properties can be estimated by microseismic fracture characterization, which permits the inference of zones prone to fracture (Refunjol et al., 2011). Although the mentioned methods permit fracture characterization, the level of detail is limited to the seismic resolution, making the estimation of the fracture size very

difficult. In areas with limited information, the LCM design should consider a range of fracture sizes rather and a specific fracture width.

3. LABORATORY MATERIALS AND METHODS

3.1 Overview

The experimental study consisted of two main stages. The first stage of experiments consisted of building a base WBM formulation with thermal stability. This formulation will serve as the foundation for a mud recipe that addresses the geothermal challenges. The main challenges are related to degradation of rheological properties and filtration and fluid loss prevention. The second stage of experiments consists of screening different LCM's to evaluate their capability of sealing fractures at HT. Besides, HT's effect in rheology tests when LCM's were incorporated into the geothermal base formula was analyzed. The main challenges are related to the thermal degradation of rheological and filtration properties. A successful geothermal mud recipe needs to satisfy different conditions low density (8.58 to 9.58 ppg), high pH (9.5 – 11.5), and the capability to maintain rheological stability at HT conditions.

3.2 Materials.

Table 11 presents the materials to be tested to find a basic formulation in the first stage of the experimental study. These materials are among the most commonly used in geothermal applications. They also were selected due to their easy availability and their relatively low cost. Those conditions are relevant since geothermal drilling operations are very cost-sensitive.

Table 11. Materials selected for 1ˢᵗ stage of experiments

Material	Property
Bentonite	Rheology Control – Viscosity Increase
Lignite	Rheology Control – Thinning Filtrate/Water loss Control
Caustic soda	Alkalinity/pH Control
Cedar Fiber	Lost Circulation

The materials presented required no preparation, except for the cedar fiber. The latter was sieved in a 600μm mesh sieve shaker. This was done to have a more homogeneous size distribution. The objective of this process is to obtain consistent results during experiments (**Figure 16**).
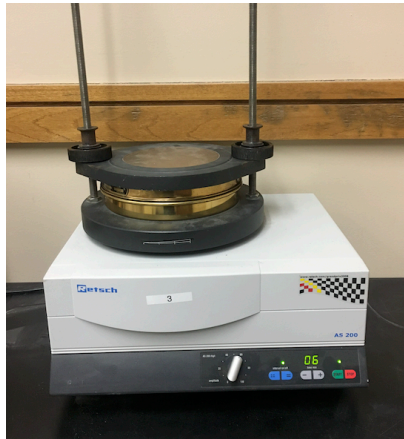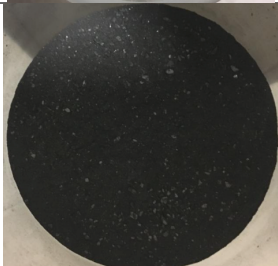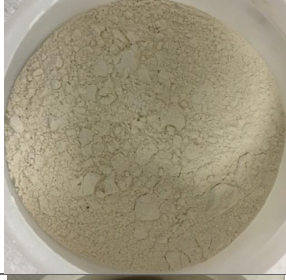
Figure 16. **Electromagnetic sieve shaker used to sieve cedar fiber.**

Table 12 presents the lost circulation materials tested. LCMs have a wide range of sizes, shapes, densities, and textures. This provides a comprehensive LCMs range to identify characteristics that made some materials more suitable to geothermal conditions than others. The materials presented are ready to use and required no preparation.

Table 12. **Materials selected for the experimental study**

Material	Type	Characteristics	Image
Walnut Fine	Granular	- Non-deformable LCM - Chemical inert - Biodegradable - SG: 1.25-1.30	

Walnut Medium	Granular	• Non-deformable LCM • Chemical inert • Biodegradable • SG: 1.25-1.30	
Sawdust	Flaky/Fibrous	• Deformable LCM • Temporary Temperature degradable • SG: 0.4-0.6	
Altavert	Fiber	• Deformable LCM • Hole sweep additive • Temporary Temperature degradable	
Graphite Blend	Granular	• Non-deformable LCM • Blend with different sizes • Torque reducing material • SG: 2.19–2.26	
Bentonite Chips	Granular	• Deformable LCM • Non-toxic • SG: 1.11-1.14 (dry)	
Micronized Cellulose (MICRO-C)	Granular	• Non-deformable LCM • Water-insoluble • Cellulosic Material	

Magma Fiber Fine	Fiber	• Deformable LCM • Acid soluble • Non-fermenting and non-corrosive • SG: 2.6	
Diatomaceous earth/amorph ous silica powder (DEASP)	Granular	• Non-deformable LCM • Silica powder • Squeeze pill design	
Cotton Seed Hulls	Fiber/Granular	• Deformable LCM • Biodegradable • Temporary Temperature degradable • SG: 0.24	
Calcium Carbonate	Granular	• Non-deformable LCM • Acid soluble • A blend of three sizes: 200, 80, and 30 CC • SG: 2.75	

3.3 Rheology Testing

All mud systems formulated were aged for 24 hours before being tested at HT. The rheometer used was a Grace instrument M5600 for measuring rheology at HPHT (**Figure 17**). The M5600 has a frictionless bob shaft construction capable of instantly measuring small changes in shear stress by a non-mechanically rotational torque signal.
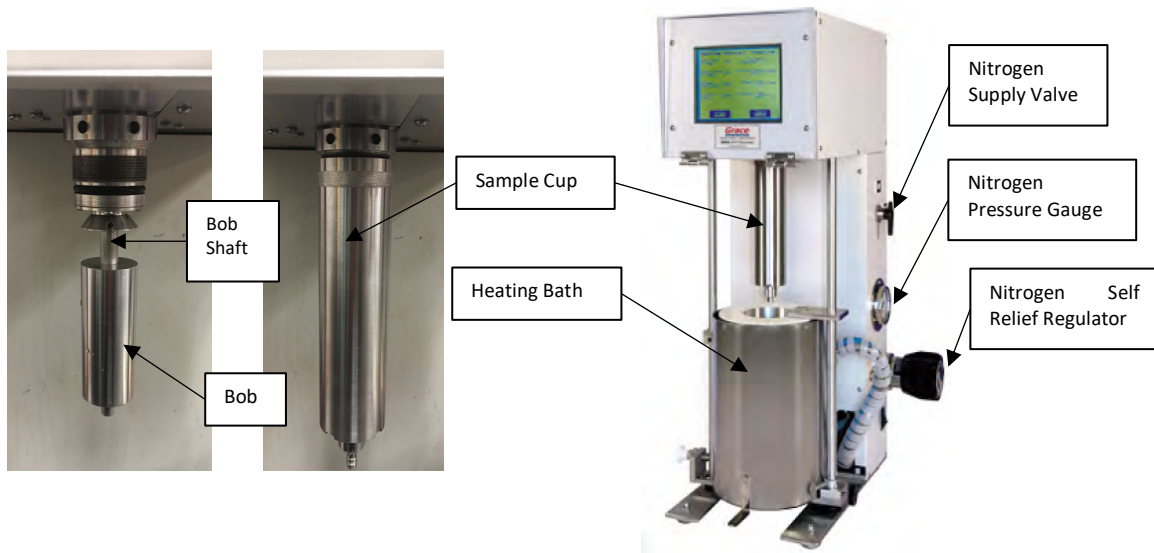
Figure 17. **M5600 Rheometer used for HPHT rheology tests.**

Figure 18 presents the schematic of the components used to perform the HPHT rheology experiments. The testing temperature was 400°F (204.5°C), and the testing pressure was 400 psi. All samples were tested using the same protocol and measurement sequence. The same scale and baker were used in all experiments to reduce the minimize divergence among results and make them comparable. The experiments were conducted two times to corroborate the results.
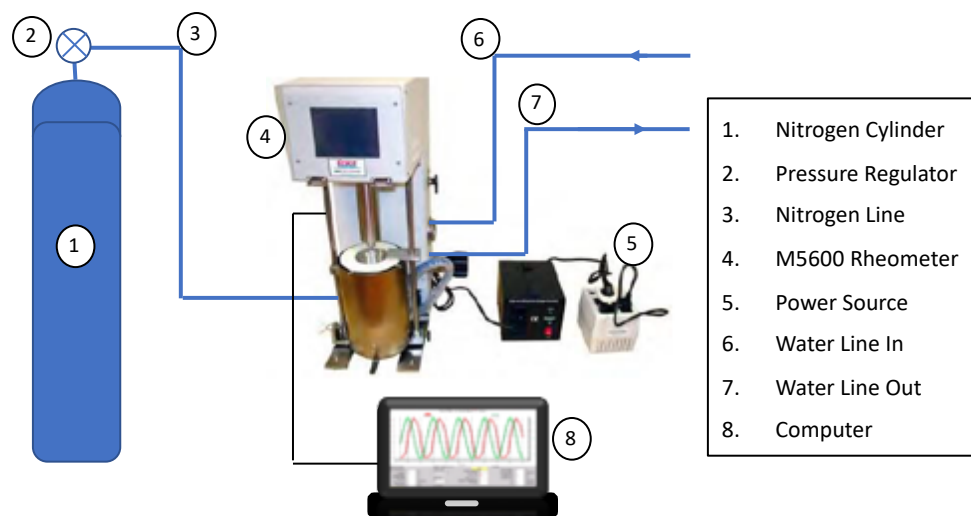
Figure 18. **Schematic of HPHT rheology test setup.**

3.4 Filtration Testing

For the static filtration tests, the equipment used was an HPHT permeability plugging tester (PPT). This equipment is designed for performing filtration tests while avoiding LCM settling. This is because the slotted disc (disc with simulated fracture) and the collecting assembly are placed at the pressure cell top. For this study, the equipment was operated at 300°F (149°C) for the LCM screening.

Different tests are performed to evaluate the effectiveness of LCM's for sealing fractures. However, they involved the usage of complex flow loops or the modification of filtration equipment. The downside of these approaches is that the results are hard to replicate or compare unless the same flow loop/equipment is used. In this research, a PPT equipment is used, with a slotted disk to simulate a fracture (**Figure 19**). The novelty of the process is using a solids-free mud; in this case, distilled water with an HPHT polymer. The polymer is a commercial polymer that ¨activates¨ with temperature, providing enough rheology to keep the LCM in suspension.
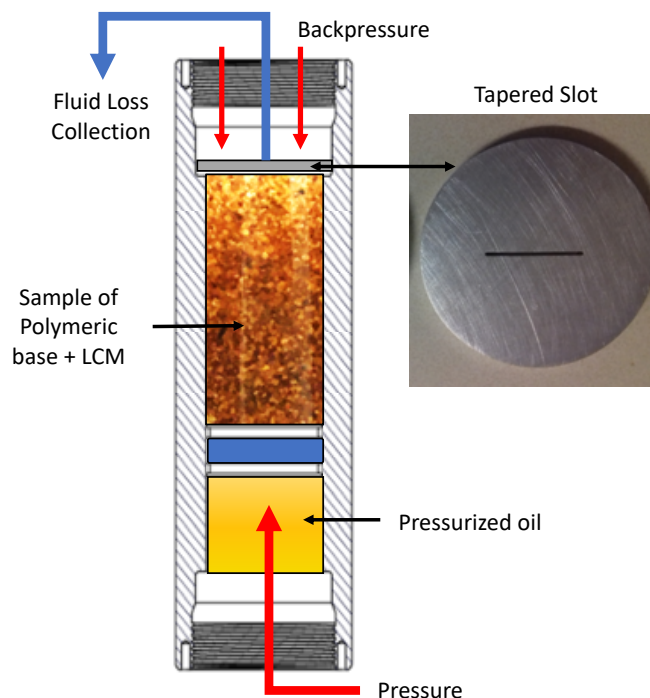
Figure 19.   Diagram of the pressure cell of the PPT apparatus for LCM filtration screening.

The advantage of using a free of solids mud for the test is that the LCMs directly generate the sealing action. This helps to provide an individual evaluation of each material sealing performance. The HPHT polymer was activated using the PPT cell, heating it to 300°F (149°C). In **Figure 20**, the mud before (a) and after (b) heating is presented. Before heating up, the mud has the minimal capability to keep LCM in suspension, then the LCM sag. After heating the mud, its rheology increased, and solids can be maintained in suspension. This is advantageous since the fluid keeps its solids carrying capacity at high temperatures in a static condition. The free of solids mud was also tested at the same conditions without LCMs showing no sealing capacity with open fractures. Then, any sealing effect in the fracture is generated by LCMs themselves. In addition, this reduces the likelihood of errors attributed to inconsistent mud preparation.

a)   b)   c)
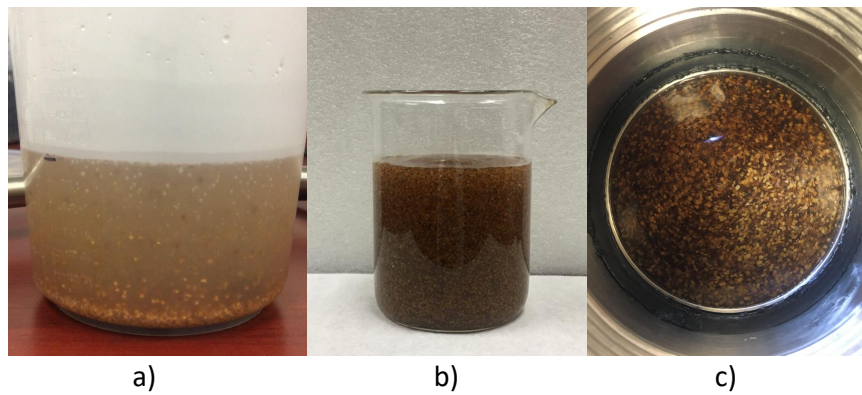
Figure 20.   Walnut fine mixed with synthetic mud; a) walnut settling in mud non thermally activated, b) walnut evenly distributed in thermally activated mud, and c) top of the PPT pressure cell filled with mud+LCM.

The mud was prepared with distilled water and 3% in weight of the HPHT polymer. The mud was then aged for 24 hours and heated up to 350°F (176.7°C) at 500 psi for activation. Once the mud is activated, it was mixed with the LCMs. The mud mixed with LCMs is aged for 24 hours before

tested in the PPT apparatus. For this initial screening, the disc with 1000μm fracture was selected to evaluate each LCMs performance, and experiments were performed twice.

The LCM's screening experiments used a similar methodology to the one presented by Savari et al. (2014). The purpose is to measure the filtration for 30 minutes. Once it is confirmed that the LCM can hold a sealing with mud pressure of 800 psi and backpressure of 300 psi, the pressure is raised by hundreds until the sealing is lost. The maximum sealing pressure obtained is recorded (this is the differential pressure of the pressure and the backpressure).

3.5 Particle Size Distribution Analysis

For fine granular materials, particle size distribution (PSD) tests were performed. The equipment used was the LS 13 320 laser diffraction particle sizing analyzer (**Figure 21**). The particle size measurement in this equipment ranges from 0.375 μm to 2000 μm. This equipment was used for measuring PSD in dry samples.

Figure 21.   **Laser diffraction particle sizing analyzer.**

3.6 Alkalinity Tests

Alkalinity control additives were also tested. To evaluate the pH buffers' performance, pH tests were performed using the PH700 Benchtop pH Meter (**Figure 22**).

Figure 22.   **pH Meter used for alkalinity tests.**

3.7   Experimental Error

Rheology and filtration experiments are exposed to errors. These errors are the expression of the different uncertainties during the experimental research's various steps, rather than the direct association to "mistakes" (Taylor, 1997).   Precision and accuracy of equipment measurements, inconsistencies in the mixing process, and human errors in reading the weight scales are examples of uncertainties during rheology and filtration experiments. Although it is inevitable to have a certain level of uncertainty, it was established some procedures to make the results conclusive in this experimental research.

For rheology experiments, the rheometer was calibrated following the manufacturer's procedure and tested successfully.

Rheology readings are sensitive to temperature changes. The HPHT rheometer has a cooling system that uses water to cool down the sample cup. For reducing the effect of room temperature changes, all samples were cooled down to temperatures below the room temperature (to 75°F /23.9°C). This step makes that all experiments have the same initial temperature.

For preparing the mud samples, the same weight scale, and beakers, and mixed the additives in the same sequence (water→gel→pH buffer→deflocculant→LCM) and mixing times. All the mud

samples were aged for 24 hours at room temperature. This is a conventional practice that permits all additives are incorporated, and bentonite absorbs water. The objective is to have more homogenous rheological properties.

For filtration experiments, it has been documented that the randomness of shape, size of the different LCM, and the random way that they are dispersed in the drilling fluid affects the tests' repeatability (Alsaba et al., 2014; Jeennakorn, 2017). Although the mentioned conditions cannot be fully controlled, to tackle this, an HPHT polymer was used as described in the filtration testing section. The usage of a solids-free mud makes the only solids in the mud are the LCM's themselves. This removes a portion of the uncertainty in this experimental research by removing the solids from other additives. Besides, as the HPHT polymer increases its rheology with the temperature increase, it maintains the LCM's in suspension, helping with a more even distribution. However, for some materials, especially the fibers, the filtration test results presented a more apparent deviation.

4. TEST RESULTS AND DISCUSSION

4.1   Overview

In this section, the results of the tests are presented and discussed. Rheology tests were performed to find which additives are best suited for geothermal temperatures. Then, a base mud formula with thermal resistance materials is found. That formulation was used to evaluate the impact on the mud rheology of different LCMs. The LCMs filtration capability was measured at high temperatures to evaluate its applicability in geothermal environments.

4.2   Drilling Fluid Rheology

To perform rheological experiments, a WBM formulation was designed. Distilled water was mixed with 20 ppb of Bentonite (20B) for rheology addition, 0.5 ppb of Caustic Soda (0.5CS) for alkalinity control, and 5 ppb of Cedar Fiber (5CF) as LCM. The MW of the sample was 8.6 ppg (1.032 sg). **Figure 23** presents the apparent viscosity at a constant shear rate (170 s^{-1}) for the samples heated up from room temperature to 400°F (204.5°C). The viscosity of the sample was relatively stable up to 200°F (93.33°C). After 200°F, rheological behavior considerably changed, showing a viscosity increase, until reaching 380°F (193.33°C). Then, the viscosity readings started to decrease. After the test was finished, the temperature was decreased to 85°F (29.5°C), and the pressure was ramped down to room pressure before removing the sample cup. Once the sample cup was removed, it was found that the mud sample had a portion that was gelled (**Figure 24**), mainly located above the rheometer bob (red rectangle in **Figure 24**). This could be an explanation for the behavior observed in **Figure 23**. As the sample was heated above 200°F (93.33°C), the viscosity began to increase, and the mud sample began to thicken. As a result of the bob rotation, part of the sample was removed from the sample cup and accumulated at the top of the bob (**Figure 24**). This reduction in the sample

cup volume causes the torque on the bob to be decreased (the friction is reduced), and the viscosity

measurement apparently decreases.
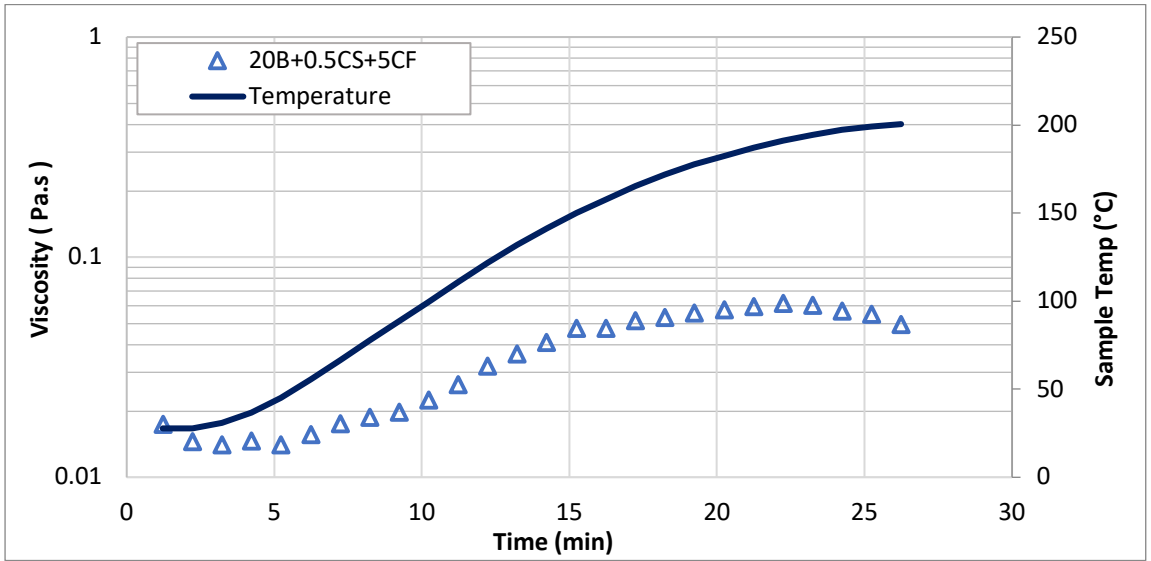
Figure 23.   **Apparent Viscosity of mud sample composed of Bentonite, Caustic Soda, and Cedar Fiber.**

Figure 24.   **A gelled portion of samples placed on top of the rheometer bob after 400°F test (left), and a portion of mud sample with a high concentration of burn Cedar Fiber in the bottom of the sample cup (right).**

Also, a low viscosity liquid portion with a high concentration of Cedar Fiber was settled at the bottom of the sample cup.

The experiments also showed a separation of a gelled portion and a liquid portion of the samples. The Cedar Fiber accumulated on the sample cup bottom could be explained by the lack of suspension capability of the degraded mud. In this case, the reduction in viscosity observed when the sample reached 380°F (193.4 °C) was probably an effect of mud gelation, rather than a reduction in the sample viscosity.

To understand the potential causes of gelation, each component of the mud was tested individually. This allows identifying their particular thermal stability and contribution to the gelation effect. The first test was performed with distilled water and 20 ppb of Bentonite concentration. An extended test was performed to replicate the effect of three "circulations". In this test, the Bentonite sample was exposed to three consecutive temperature ramp-ups. Initially, the fluid was ramped up from 85°F to 400°F (29.5°C to 204.5°C) at a constant shear rate (170 s^{-1}). The sample was then cooled down to room temperature and again ramped up to 400°F (204.5°C). This process was repeated three times to replicate the effect of temperatures ramp-up and cooling-down during drilling. This simulates the thermal stress when the mud is circulated from the surface at ambient temperature, then pumped down where it is heated up until reaching the drill bit (maximum temperature), and then cooling down when the mud flows through the annular to surface and cooled in cooling towers. The test results showed that Bentonite alone has a very high thermal stability (**Figure 25** and **Figure 26**).
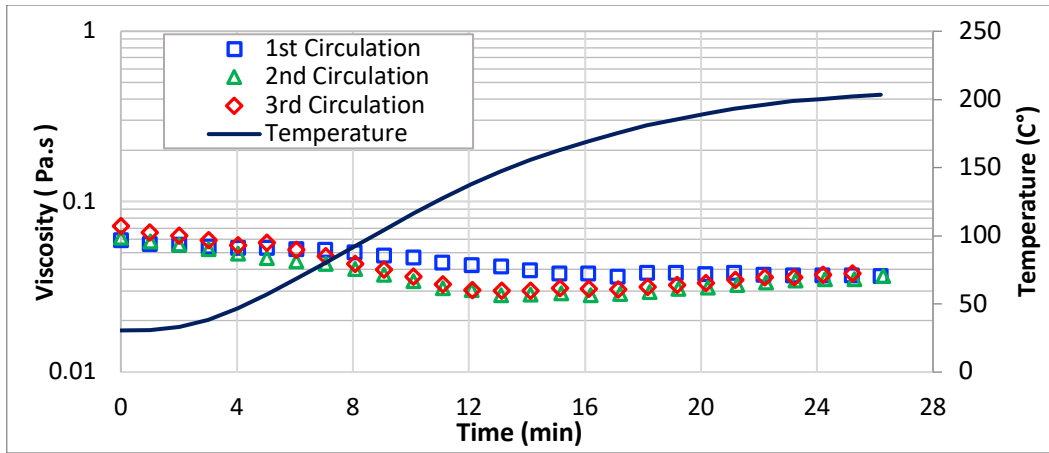
Figure 25. Apparent viscosity vs. temperature of a sample of distilled water + Bentonite (20 ppb).
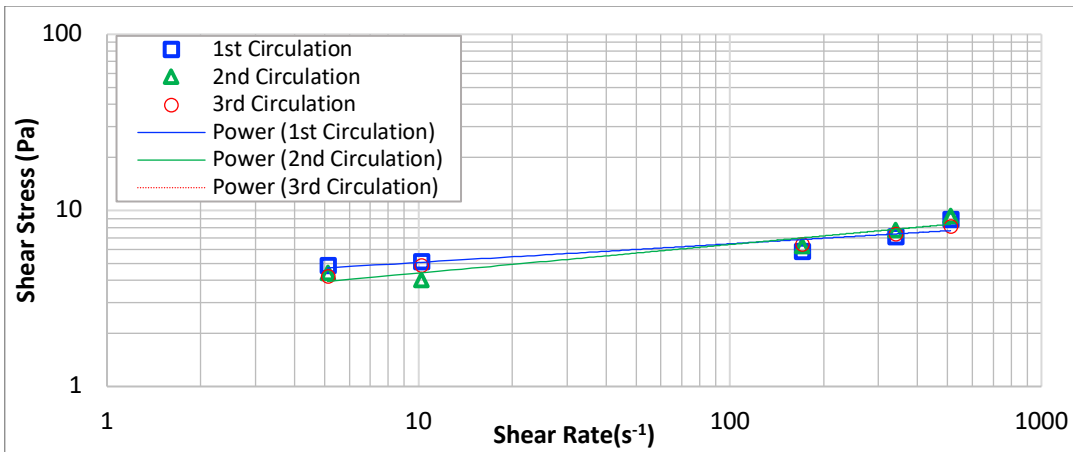
Figure 26. Rheology of a sample of distilled water + Bentonite (20 ppb).

Once Bentonite thermal stability was verified, samples of Bentonite (20 ppb) combined individually with Caustic Soda (0.5 ppb), Lignite (5 ppb), and Cedar Fiber (5 ppb) were prepared. The Caustic Soda concentration was selected due to its primary function as a pH buffer rather than its effect on the mud rheology. Increasing the alkalinity to higher values than required could have adverse effects on drilling tools and casing.

Figure 27 presented the apparent viscosity at constant 170 s^{-1} of Bentonite alone, Bentonite and Cedar Fiber, Bentonite and Lignite, and Bentonite and Caustic Soda. The results observed permit

47

indicate that Caustic Soda has poor thermal stability. At 150°F (65.6°C), the viscosity of the sample of Bentonite and Caustic Soda was around 17 cp (0.017 Pa.s), then when the temperature is increased to 350°F (176.7°C), the sample viscosity increased up to 80 cp (0.08 Pa.s). This is more than four times the previous value. This shows how this sample is sensitive to temperature increase. Additionally, the rheology test with Caustic Soda failed during readings at 400°F (204.5°C), where the rheometer rotor was staled out.
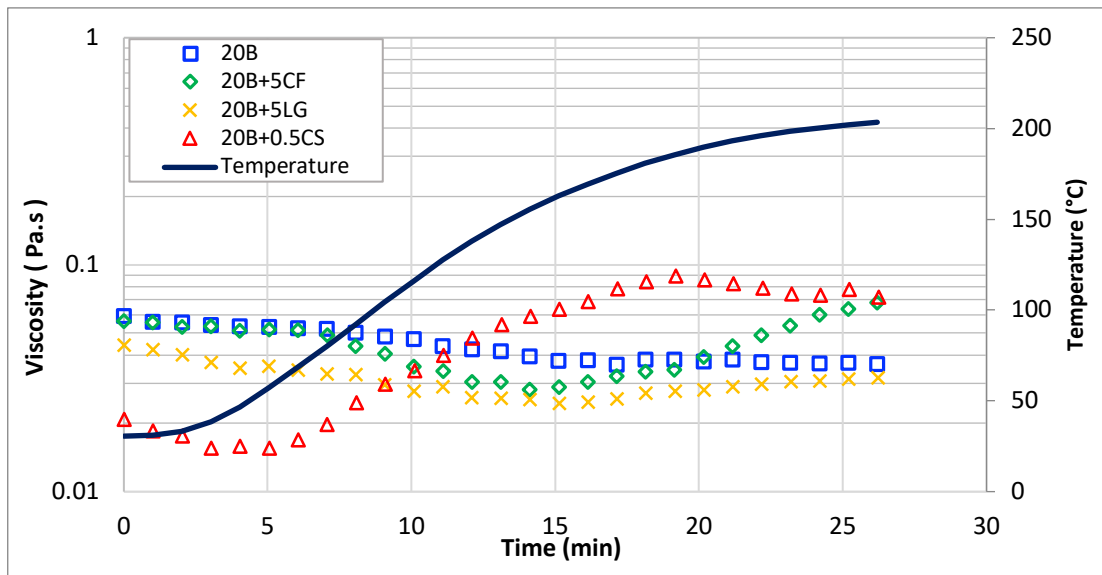
Figure 27.   **Apparent viscosity vs. Temperature and rheology of different samples.**

In **Figure 28**, the rheometer bob pictures and the liquid portion recovered after each test are presented. Sample (a) is the Bentonite alone (20 ppb), sample (b) is the Bentonite (20 ppb) with Caustic Soda (0.5 ppb), sample (c) is the Bentonite (20 ppb) with Cedar Fiber (5 ppb), and sample (d) is Bentonite (20 ppb) with Lignite (5 ppb). The sample with Caustic Soda (sample b) shows a high amount of gelled portion, with less liquid phase recovered than the other samples. This confirms the rheometer readings. The sample of Bentonite and Cedar Fiber (sample c) presented a reduction in viscosity from 56 to 25 cp (0.056 to 0.025 Pa.s) when ramped up from room temperature to 300°F (149°C). Then, the viscosity started to increase up to 68 cp (0.068 Pa.s) at 400°F (204.5°C). When

the Bentonite and Cedar Fiber sample was removed from the sample cup, we found the sample viscosity increased. However, no evidence of mud gelation was found. The Bentonite and Lignite sample (sample (d)) presented similar behavior compared with the Bentonite sample alone, suggesting they have an acceptable thermal resistance.

(a)   (b)   (c)   (d)
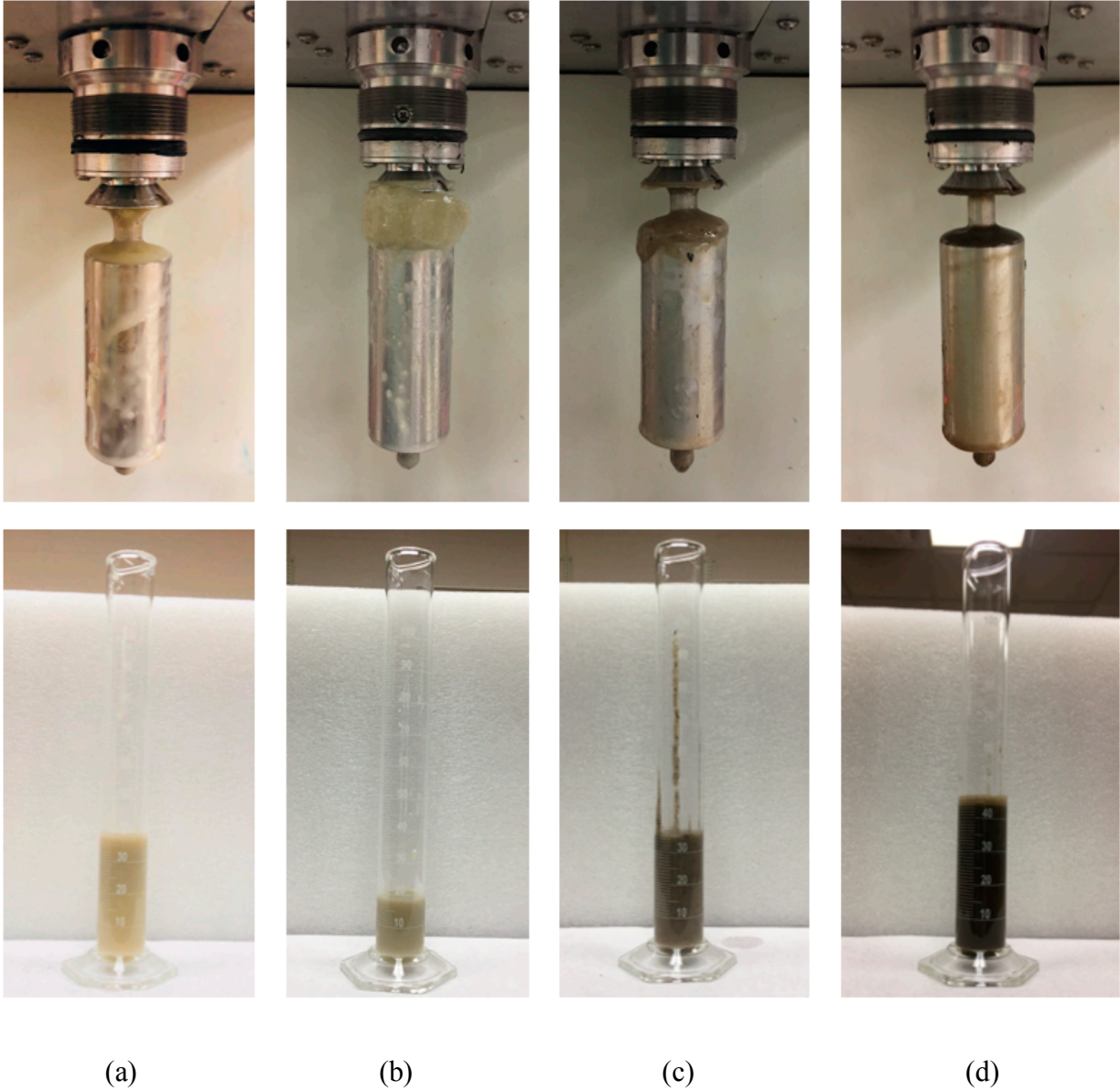
Figure 28.   Pictures of rheometer's bob and liquid portion of the samples of Bentonite alone (a), Bentonite + Caustic Soda (b), Bentonite + Cedar Fiber (c), and Bentonite + Lignite (d).

To verify if the Caustic Soda concentration has some gelation effect, samples of distilled water with Bentonite (20 ppb) and Cedar Fiber (5 ppb) were prepared. Then, caustic Soda was added at different concentrations (0.5, 1.0, and 1.5 ppb). **Figure 29** presents the apparent viscosity at a constant shear rate (170 s^{-1}) for the three samples, showing that Caustic Soda concentration has an apparent impact on mud samples rheology behavior. All three samples were relatively stable up to 200°F (93.3°C). After 200°F, rheological behavior considerably changed, showing a viscosity increase.
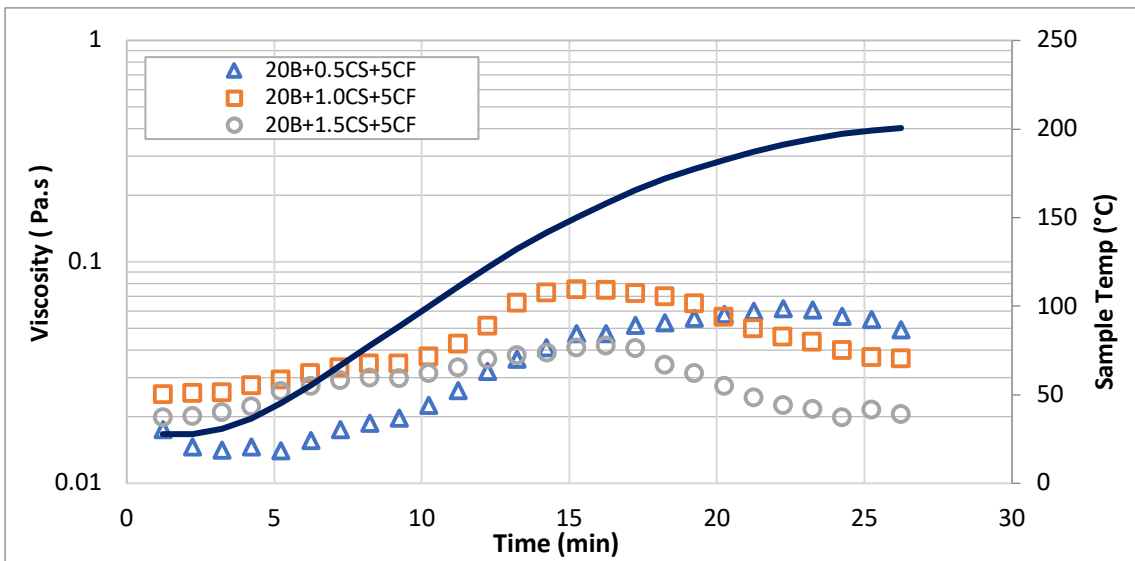
Figure 29. **Apparent viscosity of a mud sample measured at 170s^{-1} varying Caustic Soda concentration.**

The viscosity of the mud sample varies with the concentration of Caustic Soda. Although viscosity adjustments are required in some operations, using Caustic Soda for controlling viscosity is not recommended. Caustic Soda is an alkalinity control additive, and its usage to control other mud properties can lead to inadequate alkalinity values, which can trigger corrosion issues.

Besides, in operations where mud alkalinity rise would be required, the increase in Caustic Soda concentration can contribute to mud gelation. As mud gelation contributes to adverse effects as stuck

pipe events, an uncontrolled increase of ECD, or poor cementing jobs, the need for an alternative pH buffer additive has been identified.

4.2.1 Replacing Caustic Soda (NaOH) as pH Buffer.

For alkalinity control, Potassium Hydroxide (KOH), and Lime (inorganic, calcium-based mineral), are alternatives for pH regulation in geothermal drilling (Tuttle 2005). Due to their easy availability and relatively low cost, both were selected to be tested in the laboratory at geothermal conditions as potential Caustic Soda replacers.

In the first experiment, we prepared a sample of Bentonite (20 ppb) combined with KOH (0.5 ppb), Lignite (5 ppb), and Cedar Fiber (5 ppb). A long test was performed with this formulation replicating the effect of three "circulations". The same sample was exposed to three consecutive temperature ramp-ups from 85°F to 400°F (29.5°C to 204.5°C) at a constant shear rate (170 s^{-1}), then cooled down to room temperature, and again ramped up to 400°F (**Figure 30**).
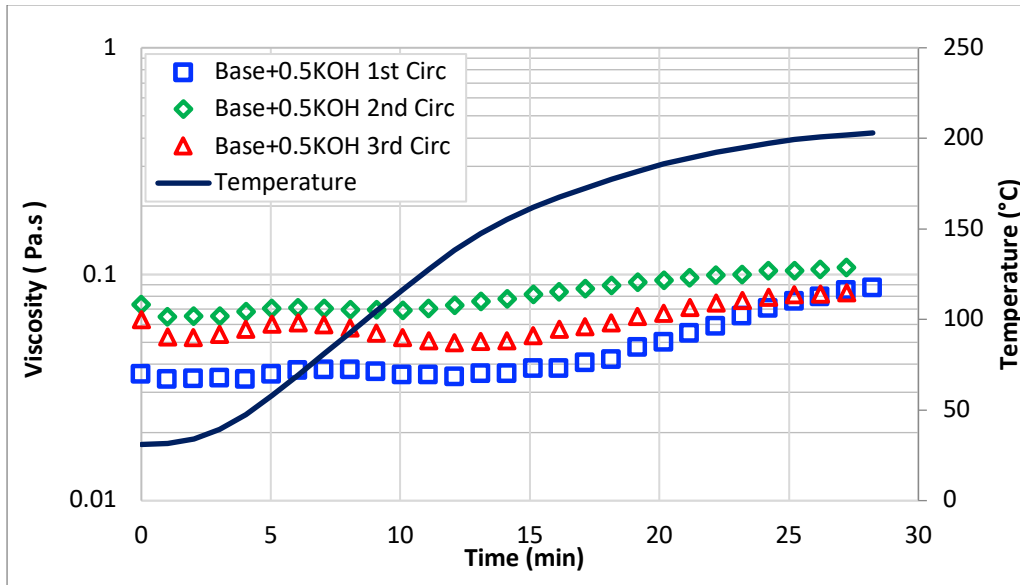
Figure 30.   Apparent viscosity vs. Temperature of WBM formulation with Bentonite (20 ppb), KOH (0.5 ppb), Lignite (5 ppb), and Cedar Fiber (5 ppb).

The results showed that the formulation with 0.5 ppg of KOH tends to increase the viscosity above 300°F (149°C). Also, at 400 °F (204.5°C), results varied among circulations. In the first circulation, the sample viscosity was 86.4 cp (0.0864 Pa.s). Then, in the second and the third circulation at the same temperature, the viscosity values were 106.8 cp (0.1068 Pa.s) and 82.5 cp (0.0825 Pa.s), respectively. Besides, during experiments, it was found that a thick and strong foam layer was formed at the mixing vessel surface once the sample was aged and stirred. This kind of foam can generate undesired effects if not controlled with defoamer.

The second alkalinity control material tested was Lime. A sample of Bentonite (20 ppb) was prepared in combination with Lime (0.5 ppb), Lignite (5 ppb), and Cedar Fiber (5 ppb). Also, an extended test was performed with this formulation replicating the effect of three "circulations". The same sample was exposed to three consecutive temperature ramp-ups from 85°F to 400°F (29.5°C to 204.5°C) at a constant shear rate ($170 \, s^{-1}$). The sample was then cooled down to room temperature and again ramped up to 400°F (**Figure 31** and **Figure 32**).
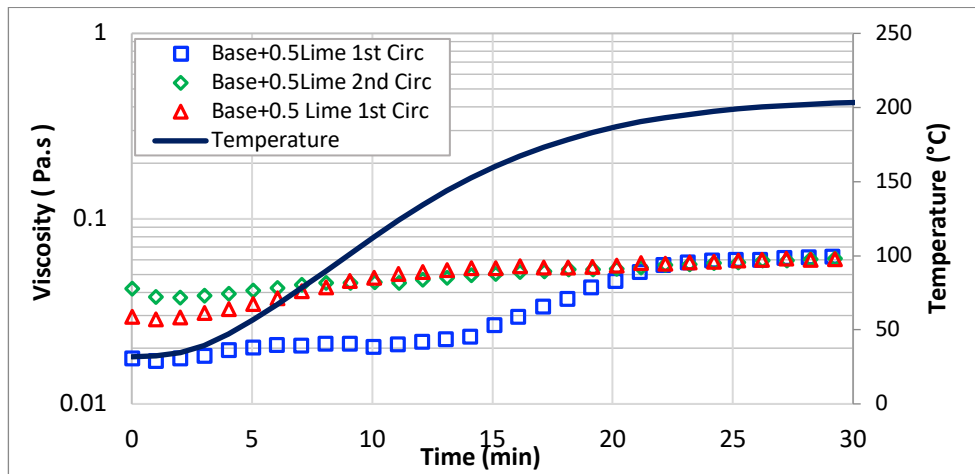
Figure 31.   **Apparent viscosity vs. Temperature of WBM formulation with Bentonite (20 ppb), Lime (0.5 ppb), Lignite (5 ppb), and Cedar Fiber (5 ppb).**
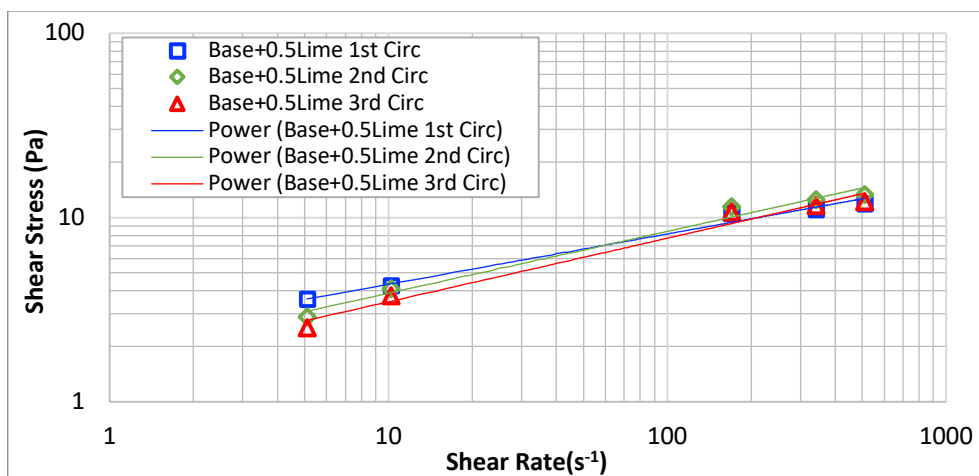
Figure 32. **Rheology of WBM formulation with Bentonite (20 ppb), Lime (0.5 ppb), Lignite (5 ppb), and Cedar Fiber (5 ppb).**

The results showed that the formulation with 0.5 ppb of Lime presents consistent values, especially after the first circulation. During the three circulations, once the sample reached the target temperature of 400°F (204.5°C), the sample becomes stable. Apparent viscosities around 60 cp (0.06 Pa.s), with a range of 2.4 cp (0.0024 Pa.s), were registered after the sample reaching 400°F (**Figure 32**). The results showed that once the sample is initially heated up to HT, it can maintain stable properties. The stability remains despite the thermal stress caused by the heating up and cooling down during the circulation process. After each temperature ramp-up, the rheology readings were taken. Consistency Index (K) and Flow Behavior Index (n) were computed at 400°F (**Table 13**). K and n values slightly decrease after each temperature ramp-up, but the decrease is not extensive. The results confirm that despite the thermal stress imposed on the sample, the rheological results remained consistent.

Table 13. **Consistency and Flow Behavior Indexes at 400°F (204.5°C) after consecutive temperature ramp-ups**

Sample	Consistency Index K	Flow Behavior Index n
Base+0.5 Lime 1st Temp Ramp-up	2.319	0.223

53

Base+0.5 Lime 2nd Temp Ramp-up	1.790	0.336
Base+0.5 Lime 3dr Temp Ramp-up	1.571	0.346

After all the experiments were performed using the Caustic Soda, KOH, and Lime, a comparison of the liquid portion recovered from the sample cup showed that Lime presented the highest recovery with 98% (**Figure 33**). This represents the portion of the sample that was not gelled. The sample with KOH presented a recovery of 66%, and the sample with Caustic Soda has a recovery of 42%. In this case, Lime is the alkalinity control material that presented the best performance.
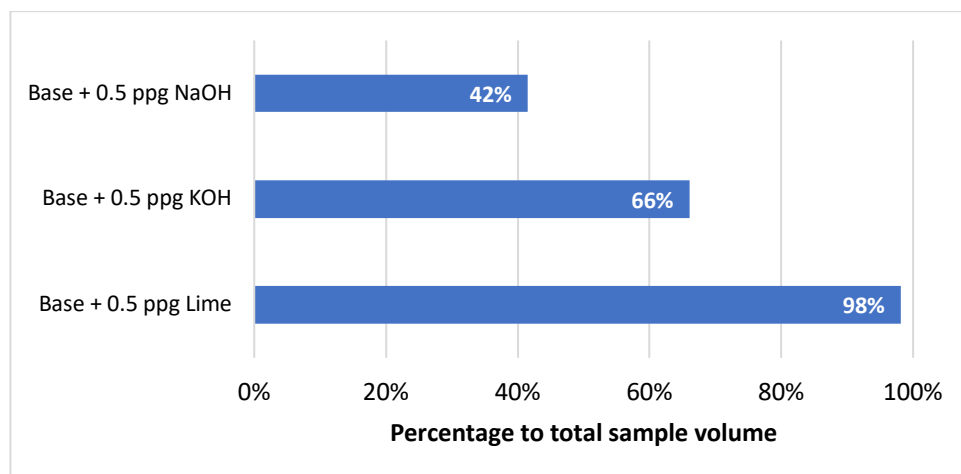
Figure 33. **Liquid Portion of Sample Recovered**

To evaluate the Lime effectiveness as alkalinity control at HT, additional rheology tests were performed. The effect of Lime concentration on long HT exposure was tested. Samples of Bentonite (20 ppb), combined with Lignite (5 ppb), and changing the Lime concentration to three different concentrations (0.5, 1.0, and 3.5 ppb), were tested. For each test, the temperature was ramped up from room temperature (80°F, 26.7°C) up to 400°F (204.5°C). Then, we maintained the temperature for 1 hour. This experiment evaluates the sample thermal stability exposed to the HT and if thermal stability remains during the time evaluated. In **Figure 34**, the test results are presented. During the

period of time evaluated, there is no major increase or decrease in the apparent viscosity, making this material suitable for the conditions tested.
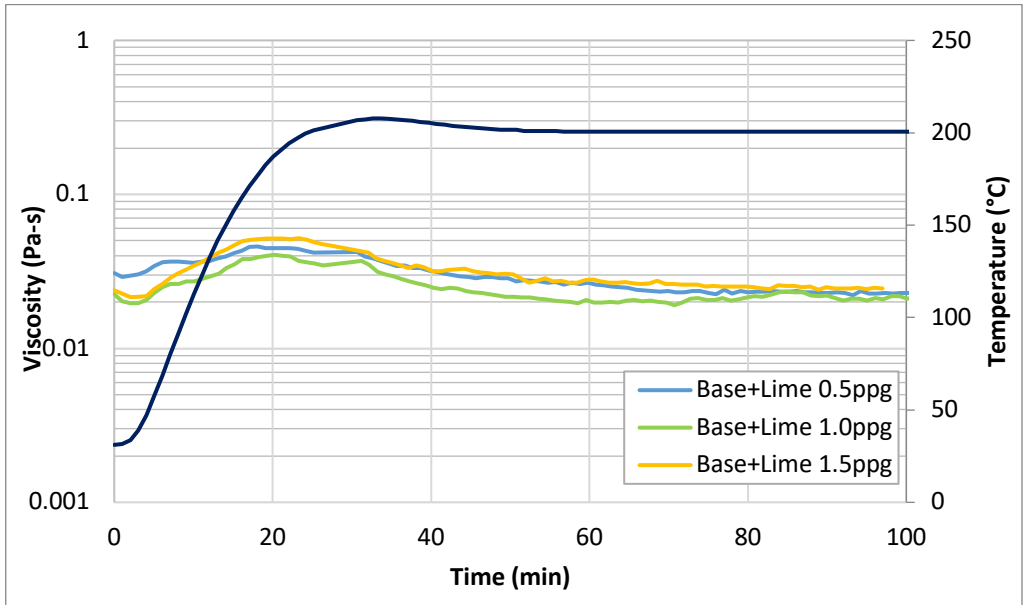
Figure 34.   **Apparent viscosity at a constant shear rate (170s⁻¹) of a base mud with 0.5, 1, and 1.5 ppg of Lime.**

Finally, to confirm the Lime capability for alkalinity control, the pH was measured in the three samples tested. In **Figure 35**, it is presented the pH test results. The Lime concentration increase has an impact on increasing the sample pH. Adding 1 ppb of Lime to the base sample+0.5 Lime increased the pH by 1.75 units, and rheology variation was just 1.6 cp (0.0016 Pa.s) at 400°F (204.5°C). In this case, Lime can adjust the alkalinity without a significant impact on the mud sample rheological behavior.
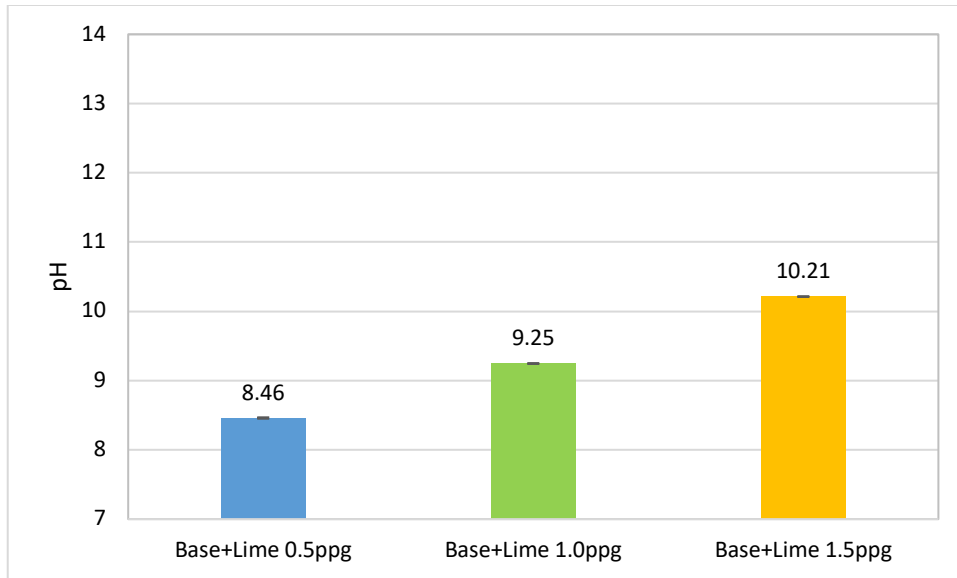
Figure 35.   **pH measurements of a base mud with 0.5, 1, and 1.5 ppg of Lime.**

4.2.2   Establishing a base WBM for High Temperatures

For establishing a base case scenario, a mud formulation with Bentonite, Lignite, and Lime (materials tested thermally stable) was prepared. The mud density was increased from 8.6 ppg to 11 ppg to avoid LCM sag during tests. Barite was added to increase the density. Besides, adding Barite permits to evaluate if the mud density can be adjusted and remain thermally stable. This base formula, without LCMs, was tested at a constant shear rate ($170s^{-1}$). The test comprises two stages; in the first stage, the temperature was ramped up from 90°F to 300°F (32.2°C to 149°C). Then, in the second stage, the temperature was maintained constant at 300°F for 1 hour. The objective is to evaluate the mud thermal stability at high temperatures. Once the sample reached 300°F and maintained HT for 1 hour, the apparent viscosity did not present major fluctuations (±4 cp to the average rheology at 300°F) (red line in **Figure 36** and **Figure 37**). This confirmed the results obtained during the previous experiments, where we tested all the base formulation components as thermally stable.

The main advantage of this thermal stable formulation (**Table 14**) is that it permits identifying the effects of the temperature on the different LCM's and its impact on rheology. Any major variation of the sample rheology can be attributed to the LCM (or the chemical interaction of the particular LCM with any of the mud components) tested in this experimental stage.

Table 14.   Additives of Base Formulation

Products	Concentration of product (ppb)	Property/Characteristic
Bentonite	25.00	Viscosifier
Lime	1.00	Alkalinity/pH Control
Lignite	5.00	Filtrate
Barite	121.2	Weighting agent

4.2.3   LCM HPHT Rheology Tests

After the establishment of a base scenario, eleven different LCM's; walnut fine, walnut medium, sawdust, Altavert, graphite blend, Bentonite chips, Micronized Cellulose, magma fiber fine, diatomaceous earth/amorphous silica powder (DEASP), cottonseed hulls, and calcium carbonate blend, were tested individually, mixed with the base formulation (**Table 15**).

Table 15.   Materials and concentration of the base formulation.

Lost Circulation Material	Type	Concentration
Walnut Fine	Granular Coarse	15 ppb
Walnut Medium	Granular Coarse	15 ppb
Sawdust	Flaky, Fiber	8 ppb
Altavert	Fiber	0.5 ppb
Graphite Blend	Granular Fine	15 ppb
Bentonite Chips	Granular Coarse	15 ppb

Micronized Cellulose	Granular Fine	5 ppb
Magma Fiber Fine	Fiber	8 ppb
DEASP	Granular Fine	8 ppb
Cotton Seed Hulls	Fiber	12 ppb
Calcium Carbonate Blend	Granular Fine	20 ppb

After analyzing the test results, a difference in the rheological behavior of coarsely granular, flaky, and fibrous materials was noticed. In **Figure 36Figure 37**, rheology tests of the mentioned materials are presented. The average percent difference between rheology readings of coarsely granular, flaky, and fibrous materials compared with the baseline is 166%. Fibrous materials, Sawdust and Magma Fiber, represent the highest variations to the baseline with 336% and 283%, respectively. Those materials also were tested prone to be gelled more than the rest of the materials. Walnuts also presented a high deviation in viscosity, with a relevant observation. Walnut Medium size LCM presented a variation of 219% to the baseline, and Walnut Fine presented a variation of 152%. Considering that both materials chemistry and physical properties are the same, the variation can be attributed to the size difference. Larger Walnut size presented a greater deviation of rheology.
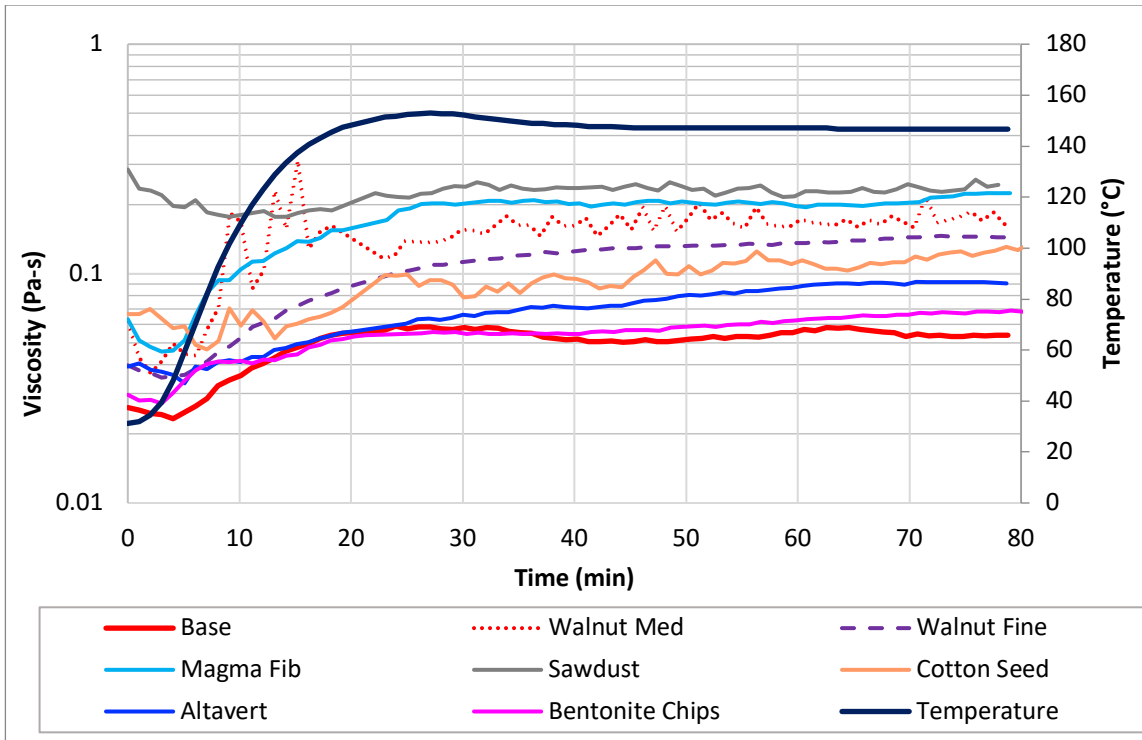
Figure 36.   Apparent viscosity of fibrous and coarse LCM's

The LCM of this group that behaves similar to the baseline was the Bentonite Chips. Initially, as this LCM is made of Bentonite, it seemed plausible that the material has a neutral effect. However, It was noticed when this material was incorporated into the mud and mixed; it started to agglomerate. The material was mechanically separated and mixed with the mud into the rheometer sample cup for the HPHT rheology test. Once the test finished, and the sample cup was disassembled, it was found that the Bentonite chips again agglomerated and stuck together on the bottom of the sample cup. As the material was found separated from the liquid portion of the sample, it is difficult to identify if the effect of the LCM in the rheology was measured or not. The Bentonite Chips concentration in the rheology test was 15 ppb. Different attempts to mix the material without agglomeration at different conditions were tried without success. Mixing the material without aging or mixing with reduced concentrations of 10 and 5 ppb was attempted. However, in all of them, the Bentonite chips agglomerated and deformed.

A group of fine granular materials was tested at the same conditions; Calcium Carbonate Blend, Graphite Blend, DEASP, and Micronized Cellulose. By contrast to coarsely granular, flaky, and fibrous materials, the fine granular materials behave similarly to the base case (**Figure 37**). The average deviation of the materials tested to the baseline was 17.6%. The mentioned products do not show that they significantly alter the base fluid rheology. Besides, no evidence of mud gelation was observed. It is possible to infer that these materials are more thermally resistant at the tested temperatures than coarse, flaky, and fibrous materials.
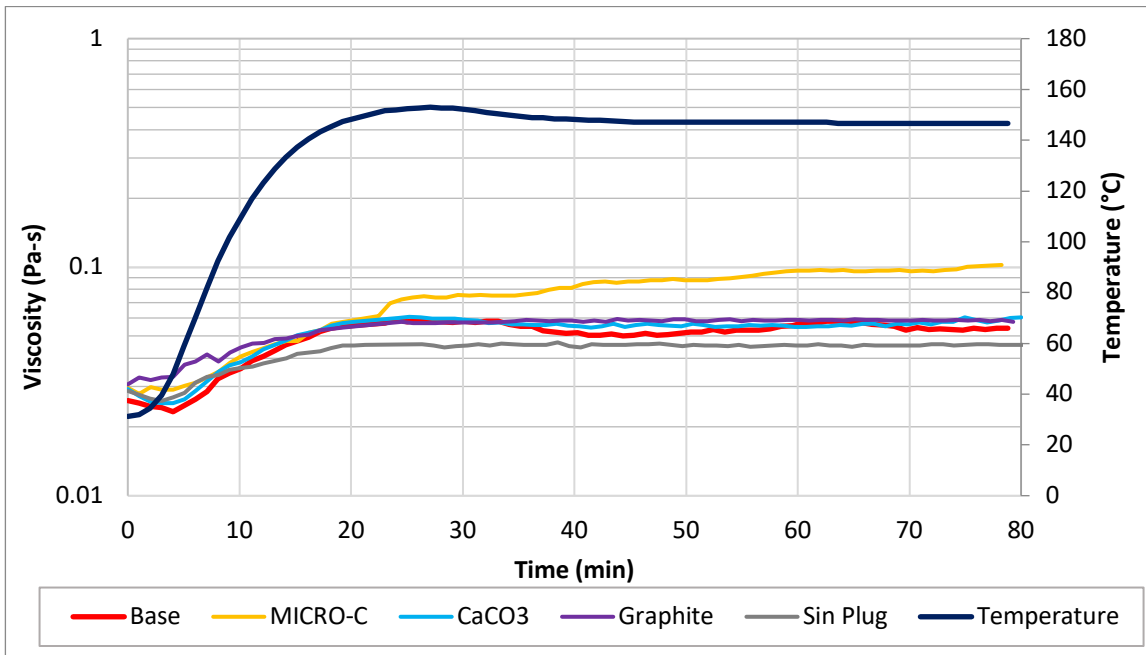
Figure 37.   Apparent viscosity of fine granular LCM's.

To better understand the influence of LCM's particle size, a PSD (Particle Size Distribution) experiment was performed on fine granular materials. The PSD equipment measures particles from 0.375μm up to 2000μm. In **Table 14**, the test results on calcium carbonate blend, DEASP, Micronized Cellulose, and graphite blend are presented.

Table 16.   Summary of PSD test on various LCM's

Variable	CaCO3 Blend	DEASP	Micronized Cellulose	Graphite Blend
From (μm)	0.375198	0.375198	0.375198	0.375198
To (μm)	2000	2000	2000	2000
Volume	100	100	100	100
Mean (μm):	165.78	15.67	505.66	761.21
Median(μm):	88.24	11.21	406.97	717.12
Mean/Median ratio:	1.88	1.40	1.24	1.06
Mode (μm):	390.96	13.61	623.27	1908.87
S.D. (μm):	186.50	18.66	452.19	632.72
Variance ($μm^2$):	34782.60	348.30	204476.00	400336.00

It is observed that the LCM with the smallest mean size, The DEASP, also presented the lowest average apparent viscosity at 300°F (149°C), with a value of 45.6 cp (0.0456 Pa.s). CaCO3, with a mean size of 165.75μm, and Micronized Cellulose with a mean size of 505.66μm, presented average apparent viscosities at 300°F of 56 cp (0.056 Pa.s) and 91.5 cp (0.091 Pa.s) respectively. This shows the influence of size in rheological readings at HT. The mean size of Graphite Blend is the largest of the granular materials tested. However, the average apparent viscosity at 300°F is very close to the baseline (58.5 cp (0.0585 Pa.s)). This can be attributed to the Graphite lubricity. The effect lubricity of a graphite-based LCM was also documented by Alsaba et al. (2014).

4.2.4   Discussion

Considering the geothermal drilling challenges, incorporating additives to control density, viscosity, alkalinity, filtration, and fluid loss are fundamental. However, the simple act of putting together additives to meet those functions does not guarantee a successful application in geothermal operations. Some additives thermal degradation has an apparent effect on the drilling fluids rheology

and identifying which fluid components of the mud formulation are originating gelation has not been widely studied.

In this case, it is worthwhile to evaluate the effects of certain components individually in the drilling fluid rheology when exposed to high temperatures. This may help identify some of the characteristics that made some additives more sensitive to temperature changes than others.

In this experimental work, Bentonite rheological behavior was evaluated at high temperatures, finding no mud gelation evidence. Two of the most common additives used in geothermal applications, Caustic Soda (alkalinity control) and Lignite (filtration, deflocculation), were tested. It was identified when Caustic Soda is mixed with Bentonite and exposed to temperatures above 200°F (93.3°C), mud gelation begins to occur.

Two materials were tested as potential replacements for Caustic Soda; Potassium Hydroxide and Lime. In HPHT rheological experiments, Lime showed better thermal stability than KOH and Caustic Soda.

We initially tested the LCM effect with a Bentonite and Cedar Fiber sample, showing that LCM also influences rheology at high temperatures. As diverse LCM additives have been used in geothermal drilling with diverse characteristics and properties, we selected 11 different LCM materials to cover different alternatives.

After analyzing the HPHT rheological experiments results, we identified that materials that performed better were fine granular materials compared with coarse larger-sized granular materials and fibers. The probable reason is that smaller particles have a larger surface area per unit of mass, meaning that the heat is distributed in a larger surface area at high temperatures, making these materials more thermally stable.

4.3 Filtration Tests

One of the main objectives of this experimental study is to understand the effect of high temperatures on LCM's performance. In the previous experimental stage, it was found that increasing temperatures to values equal to or above 300°F (149°C) affect the rheology of some LCM. This suggests that the exposure of some LCM to high temperatures generates a change in the materials themselves. This change caused by the high temperature in some LCM can potentially affect sealing and bridging fractures' effectiveness. Hinkebein et al. (1983) found experimentally that temperature increase reduces the sealing pressure of some cellulosic LCM's. In **Figure 38** it is presented a comparison test performed with the base mud with cedar fiber (5 ppb) at 120°F (49°C) and 300°F (149°C).
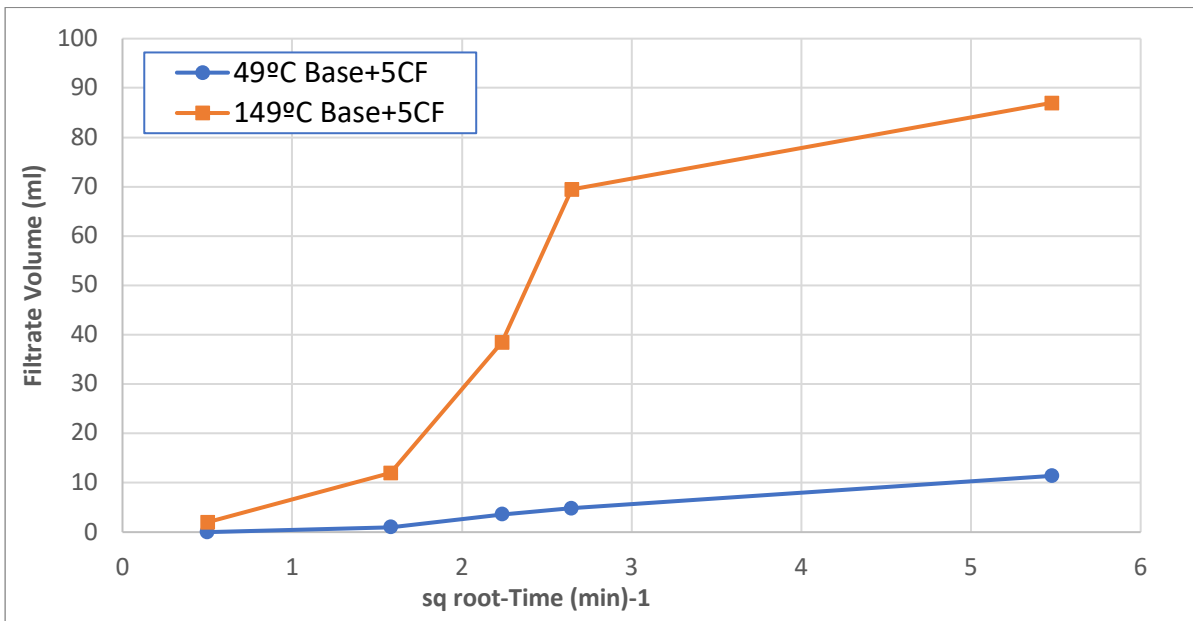
Figure 38.   **Filtration test perform with a base mud (Bentonite, Barite, Lignite and Lime), and Cedar Fiber with a 5 ppb concentration.**

The results show how the sealing capability is reduced at high temperatures. However, as the higher temperature test take longer before filtration start, it was also suspected that material sagging could

63

affect the results. For that reason, the filtration tests for screening LCM's were performed as described in section **3.4**. The advantage to performing the filtration experiments using a solids-free mud formula is that all solids in the sample come from LCM's themselves. Besides, as the HPHT polymer is HT resistant, once activated, it maintains its rheological properties. This helps to reduce the LCM's sagging during the extended high-temperature tests.

In **Figure 39**, the 30 minutes filtration profile results of the different tests are presented. The LCM's that performed best were MICRO-C, calcium carbonate blend, and graphite blend. The similarity between these materials is that they are granular, with small particle size, and all of the three are blends, so they have a wide range of particle size.
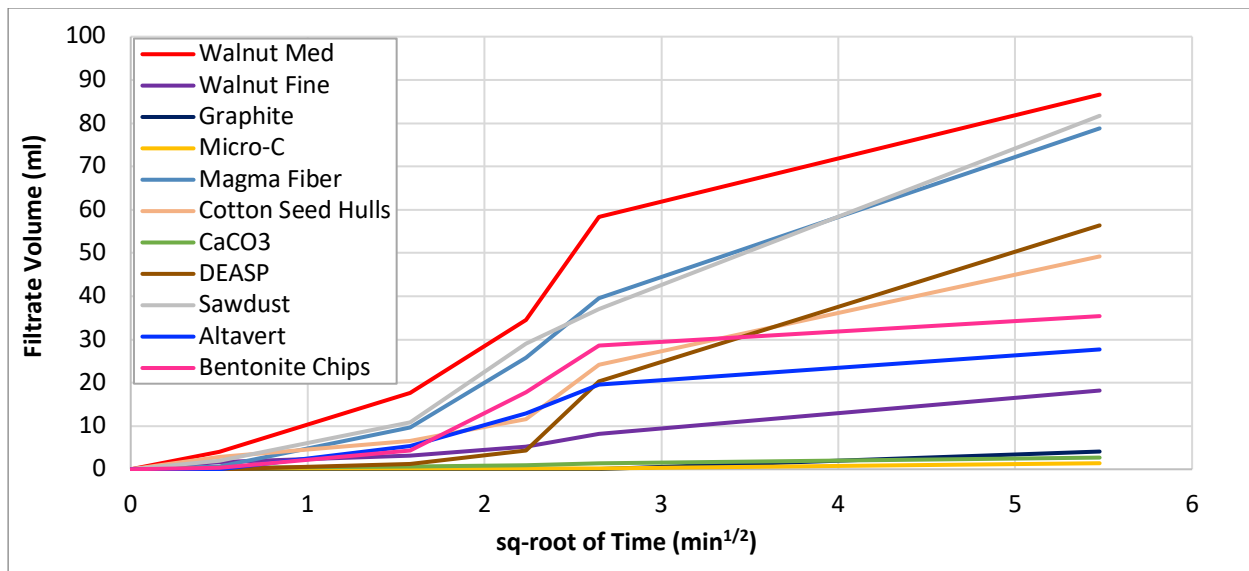
Figure 39. **Filtration results of individual tests of the free of solids mud + LCMs**

In **Figure 40**, it is presented the 30 minutes filtration tests and the maximum sealing pressure for each LCM. The maximum sealing pressure was obtained by the graphite blend, calcium carbonate, Altavert, and MICRO-C.
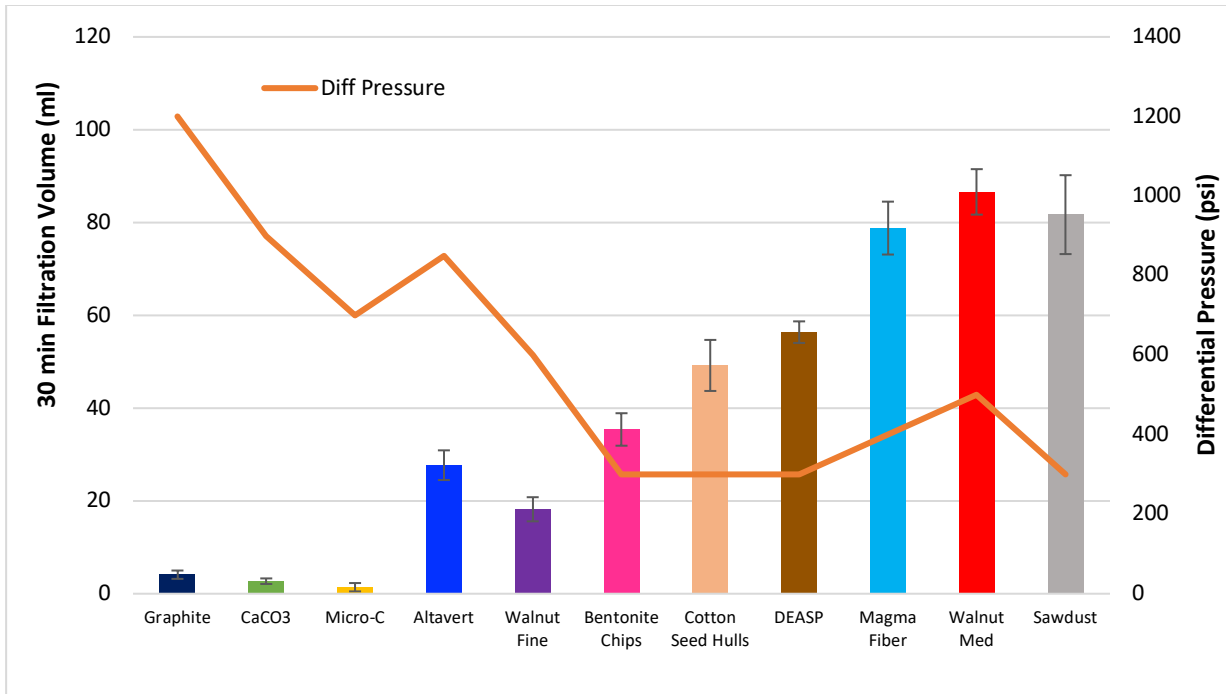
Figure 40. **Filtration volume and maximum sealing pressure obtained of different LCMs**

It was observed that the deviation among filtration tests is more apparent in fibrous materials, such as Sawdust, Magma Fiber, and Cotton Seed Hulls. In contrast, the fine granular materials present more uniform results.

Figure 41 showed a close-up view of the 1000μm fracture of the three materials that performed best in the filtration experiment. The three LCMs successfully sealed the fracture without other solids. The graphite blend was the only LCM that reached the maximum sealing pressure of 1200 psi. This value could be higher, considering that the maximum mud pressure was limited to 1500 psi for safety reasons (and the backpressure was a constant 300 psi). The Calcium Carbonate blend provided a sealing pressure of 900 psi. When the pressure was increased above 900 psi, the sealing pressure was suddenly lost, and it was not possible to recover it back. The MICRO-C sealing pressure was 700 psi. When the sealing pressure was increased above 700 psi in the MICRO-C test, the sealing pressure was reduced gradually, but with time, the sealing was recovered, and pressure could be

increased again to 700 psi. This effect can be visualized in **Figure 41**, where it can be seen that in the CaCO3 experiment, the seal was lost, and the fracture is open. In contrast, the MICRO-C sealing was maintained. This effect can be attributed to the deformability of MICRO-C and the non-deformability of CaCO3.
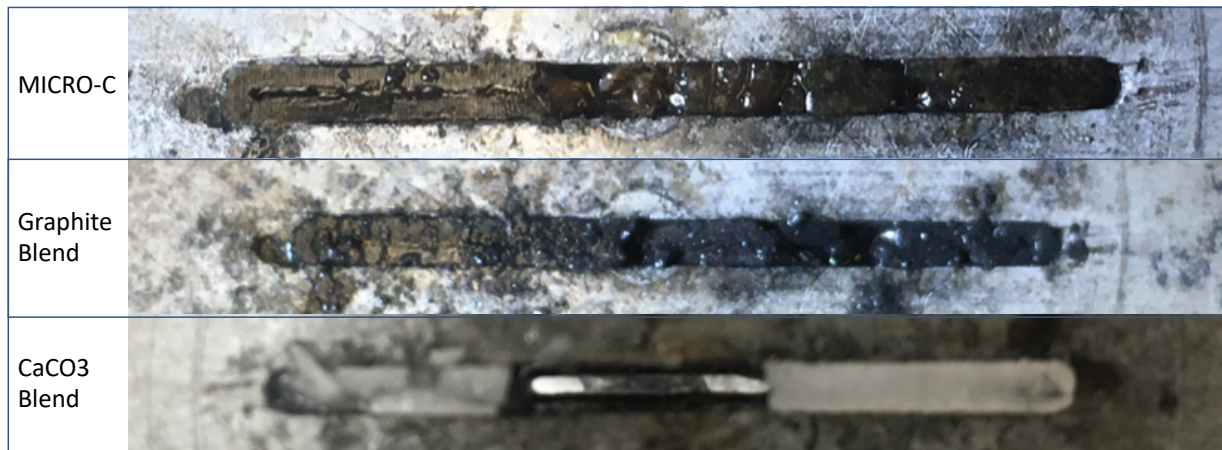
Figure 41.   Close up view of 1000μm fracture once the disk was removed from the pressure cell.

4.3.1   Particle Size Distribution Tests

To better understand the influence of LCMs particle size, a PSD (Particle Size Distribution) analysis was performed on fine granular materials. The PSD equipment measures particles from 0.375μm up to 2000μm. **Figure 42** and **Figure 43** show the test results on calcium carbonate blend, DEASP, MICRO-C, and graphite blend.
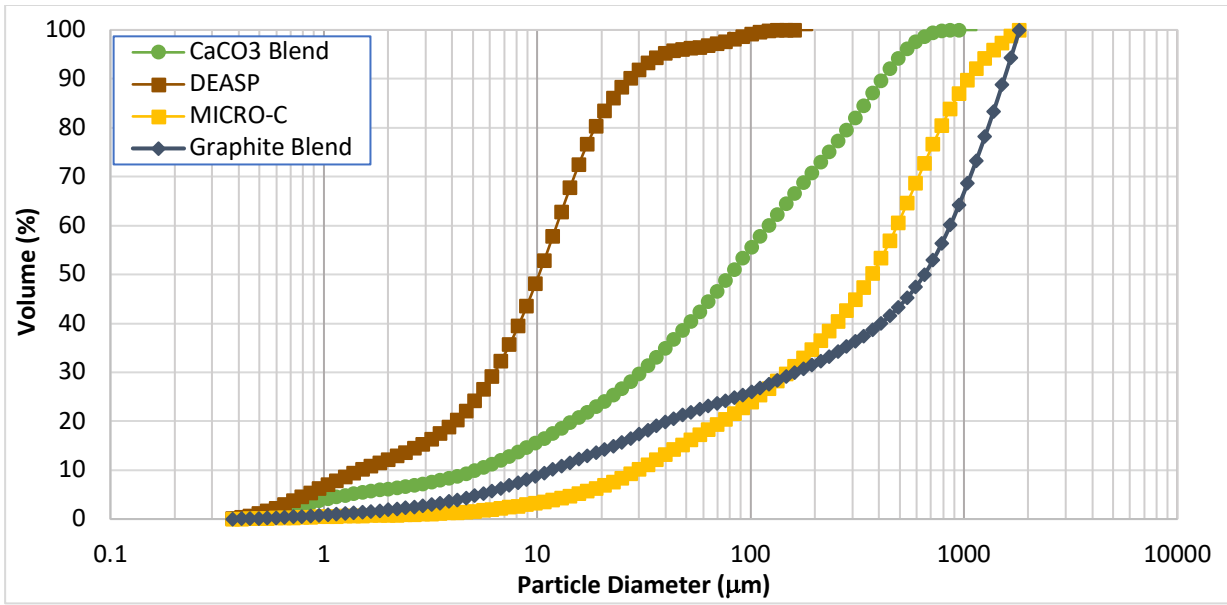
Figure 42. PSD test on different fine granular LCM's
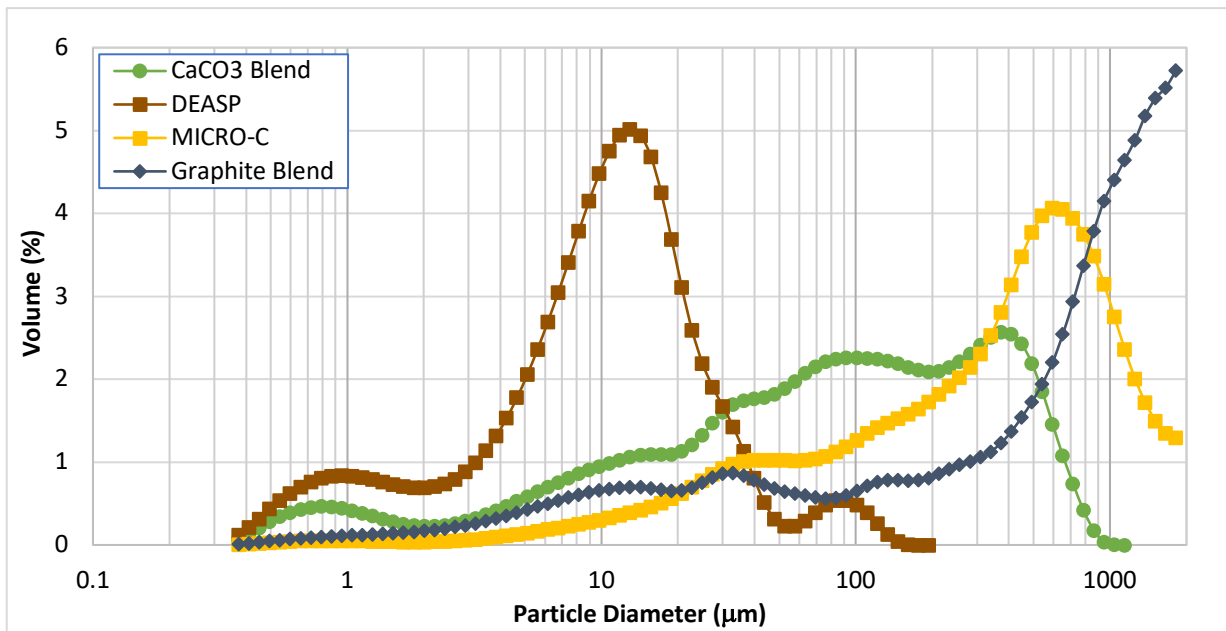
Figure 43. Frequency curve of particle diameter test on different fine granular LCM's

As it can be observed in the PSD analysis, the DEASP curve shows a Gaussian distribution of the values (bell shape), and the other materials presented a wider range of particle diameters with their curves right-skewed. To determine the PSD influence on the filtration performance, the filtration results of the components analyzed are presented in **Figure 44**.

67
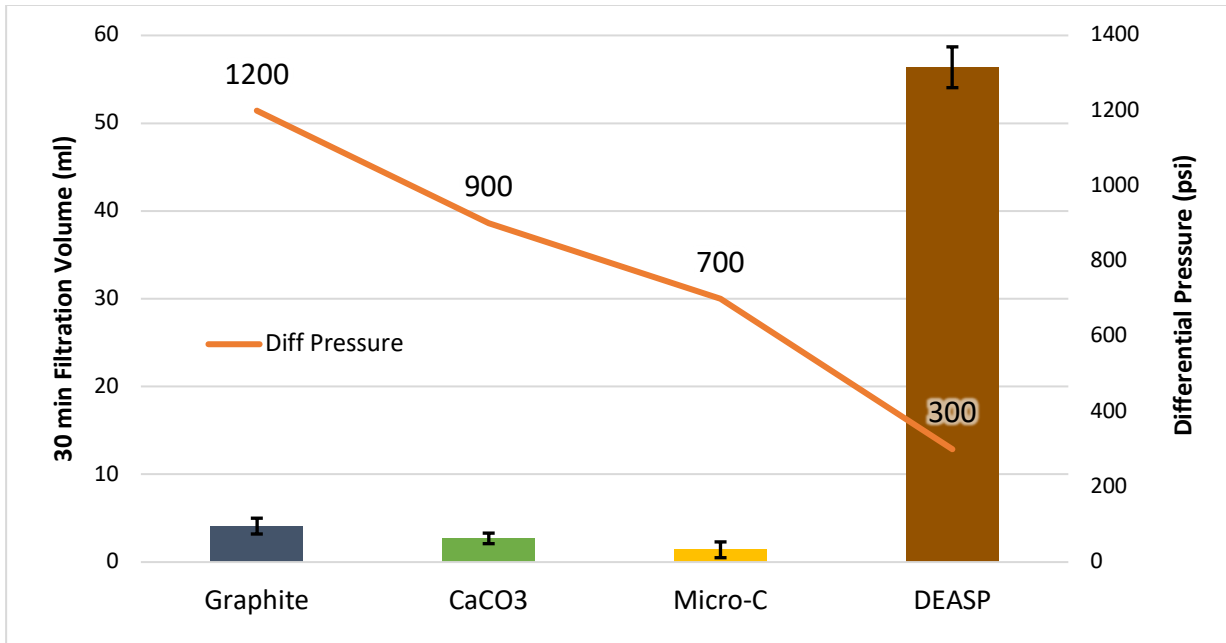
Figure 44. **Filtration and differential pressure results of fine granular LCMs tested.**

According to the filtration results, the materials with a wider particle size distribution (graphite blend, calcium carbonate, and MICRO-C) showed the best filtration performance. In contrast, the DEASP, the granular material with a narrower particle diameter values range, had a higher filtration volume. Having a wide range of particle sizes is a desirable condition in an LCM for sealing fractures; larger grains can build the bridge, creating support for the smaller particles that generate the effect of sealing. In **Table 17**, it is summarized the PSD test values. The mean diameter of the DEASP is 15.67 μm, which is significantly smaller than the average diameters of the other LCMs analyzed.

Table 17. **Summary of PSD test on various LCM's**

Variable	CaCO3 Blend	DEASP	MICRO-C	Graphite Blend
From (μm)	0.375198	0.375198	0.375198	0.375198

To (μm)	2000	2000	2000	2000
Volume	100	100	100	100
Mean (μm):	165.78	15.67	505.66	761.21
Median(μm):	88.24	11.21	406.97	717.12
Mean/Median ratio:	1.88	1.40	1.24	1.06
Mode (μm):	390.96	13.61	623.27	1908.87
S.D. (μm):	186.50	18.66	452.19	632.72
Variance (μm^2):	34782.60	348.30	204476.00	400336.00

4.3.2 Discussion

After analyzing the experimental results, it was identified that materials that performed better in the filtration tests were fine granular, blended materials. This does not necessarily mean that they are the best materials for all applications. However, the testing conditions show that those materials are suitable for geothermal environments.

Fine granular materials behave better at high temperatures compared with coarse larger size granular materials and fibers. A reasonable argument is that smaller particles have a larger surface area per unit of mass. This means that the heat is distributed in a larger surface area at high temperatures, making these materials more thermally stable. That indicates small granular materials can keep their sealing properties at HT better than fibers and coarse materials.

For sealing a fracture, it is beneficial to have a large size range. Larger particles create a permeable bridge, and the smaller particles fill out the bridge spaces to build a seal. This can explain why LCMs like calcium carbonate and graphite blends or MICRO-C, with a wide range of particle diameters,

worked better than the DEASP. The variance of DEASP ($348.3\mu m^2$) is significantly smaller than the variance of the other LCMs that present the best performance in the filtration tests.

As the filtration tests were performed with a free of solids mud, all the sealing action came from each LCM. However, in practice, drilling fluids contain solids from the mud additives and the drilling cuttings. The mentioned solids also contribute to the fracture sealing process.

The ratio between the size of the fracture and the particle size is another important factor to consider. In **Table 18**, it is summarized the particle size distribution of the fine granular materials analyzed. Considering those values, the particle sizes were evaluated based on the different particle size criteria used in the industry (**Table 10**). The results presented in **Table 19** are the values computed based on each specific condition.

Table 18.   **Summary of PSD analysis for fine granular materials.**

Material	Fracture Size	D10 μm	D25 μm	D50 μm	D75 μm	D90 μm
CaCO3 Blend	1000 μm	5.71	24.42	88.24	256.31	456.51
DEASP	1000 μm	1.65	5.81	11.21	18.21	29.87
MICRO-C	1000 μm	32.59	119.47	406.97	758.07	1153.87
Graphite Blend	1000 μm	12.77	95.11	717.12	1297.28	1696.26

Table 19.   Summary of application of particle size selection methods based on the material's PSD results.

Method	**Selection Criteria**	**CaCO3 Blend**	**MICRO-C**	**Graphite Blend**	**DEASP**
Abrams Rule (Abrams 1977)	D50 ≥ 1/3 the formation average pore size	No	Yes	Yes	No
D90 Rule (Smith et al. 1996, Hands et al. 1998)	D90 = the formation pore size	No	Yes	Yes	No
Vickers Method (Vickers et al. 2006)	D90 = largest pore throat	No	Yes	Yes	No
	D75 < 2/3 the largest pore throat	Yes	No	No	Yes
	D50 ≥ 1/3	No	Yes	Yes	No
	D25 = 1/7 the mean pore throat	No	No	No	No
	D10 > the smallest pore throat	-	-	-	-
Halliburton Method Whitfill, 2008	D50 = fracture width	No	No	No	No
Alsaba Method (Alsaba et al.2016)	D50 should be ≥ 3/10 the fracture width	No	Yes	Yes	No
	D90 should be ≥ 6/5 the fracture width	No	Yes	Yes	No

There are no selection criteria from **Table 19** that calcium carbonate blend, graphite blend, and MICRO-C together completely meet. Graphite blend meets most of the conditions of the different

selection criteria presented. MICRO-C also meets most of the criteria except Vickers and Halliburton Methods. For Halliburton Method, the criteria in the D50 is 1000μm, and no one of the materials tested satisfy that criterion.

Sealing a fracture involves the LCM's ability to build a bridge inside the fracture. The D90 size is considered in some of the recent selection criteria. The D90 includes the largest size particles, destined to bridge the fractures. As observed, MICRO-C and graphite blend met some of the D90 size criteria methods used in the industry. However, the calcium carbonate blend, LCM that showed a good performance in the filtration test, did not meet most of the criteria methods.

Calcium Carbonate blend has a D90 size of 456.51 μm, close to half of the fracture width size (1000μm). Since Calcium Carbonate successfully sealed the fracture, the D90 size value in some of the selection criteria could be re-evaluated in the future.

This suggests that 10% of the particles with size near the half of the fracture are enough to build the bridge into the fracture. Then it is possible to distribute the remaining 90% to create a wider range of particle size. Once the bridge is built, a wider range of smaller particles will fill the permeable bridge spaces to generate the sealing.

This is an important condition since, in geothermal applications, large fractures are frequently found. In this case, materials with greater particle size need to be included. However, if the particle size is unnecessarily large, they will become prone to degrade/fail at high temperatures.

According to the experimental results, we suggest that size selection criteria must have at least two conditions. The first is that the D90 has enough size to build the bridge. The second condition is that LCM needs to have a large size distribution. This will help to generate the seal. This experimental

research suggests that the PSD variance could be considered to guarantee a large particle distribution.

5. SUMMARY AND CONCLUSIONS

High temperatures affect the rheology of WBM. These drilling fluids formulations commonly use Bentonite as a viscosifying agent and additives to improve rheology, filtrate control, and pH. To identify how thermal degradation is manifested, drilling fluid additives have to be tested individually at HT. The followings are the outcomes of this study:

- In literature, it is claimed that bentonitic fluids tend to gel at high temperature. However, in this research, we found that Bentonite itself has high thermal stability. In accordance, it is recommended to continue using Bentonite as a viscosifier for geothermal drilling fluids due to its thermal stability, easy accessibility, and low cost.

- Caustic Soda, the most common additive to control pH, presented poor thermal stability, evidencing a tendency to gel at temperatures above 200°F (93.3°C).

- After evaluating Lime and KOH as potential substitutes of Caustic Soda, we found it via experiments at geothermal conditions that Lime is the alkalinity control material that presented the best performance in rheological stability at high temperatures.

- A basic formula consisted of water, Bentonite, Lime, and Lignite was tested at high temperatures, showing adequate thermal stability. This basic formulation can be adjusted in density using Barite, remaining thermally stable.

- The lost circulation materials that performed better in the HPHT rheology tests were fine granular materials. These materials showed less rheology impact in the base mud formulation than the impact caused by coarse larger-sized granular materials and fibers.

- We found experimentally that the particle size of LCM materials has a direct influence on the rheology when tested at HT.

- A methodology of screening lost circulation materials is presented by an innovative way to use the PPT at high temperatures. The usage of free of solids mud permits to determine the capability of different LCMs to seal an open fracture at HT. Besides, their sealing pressure can be measured in controlled conditions.

- It was identified that materials that performed better in the filtration tests to seal the 1000μm fracture were granular, blended materials. Graphite blend, MICRO-C, and calcium carbonate blend sealed the 1000μm fracture, generating higher sealing pressure compared with other materials.

- Based on the experimental findings, it is recommended that the size selection criterion must have at least two conditions. The first is that the D90 is big enough to create a bridge. The second criterion is that the LCM should have a wide size distribution. This is going to help create the seal. This experimental research indicates that the PSD variance may be considered a guarantee of the large particle distribution needed.

- Experimental research at high temperatures is helping us to identify materials that work best than others. Size, shape, and particle size distribution impact the filtration capability of LCM.

The conclusions presented were based on observations made during this research and applied to the different mud samples used in the analysis. It is important to remember that muds with different additives concentrations can have varying responses to high temperatures. However, the general behavior of mud is assumed to be roughly comparable.

6. RECOMMENDATIONS AND FUTURE WORK

This study presented experimental research on how HT affects the performance of different drilling fluid additives. Some of the outcomes of this study suggest further research that can improve how to design a drilling fluid capable of addressing geothermal drilling challenges.

- Conduct experiments using different fracture sizes. This, combined with the particle size distribution results, will provide new information to generate new size distribution criteria for HT/Geothermal applications.

- Generate an HPHT filtration experiment in dynamic conditions. With some adjustments, the drilling simulator setup in the Well Construction Technology Center (WCTC) can be used to conduct those experiments.

- Screen the fine granular LCM, adding drilling cuttings to the drilling mud to evaluate their impact.

- Similarly, evaluate the implementation of nanoparticles. This especially could impact the sealing pressure.

- Conduct experimental research using shape memory polymers as a filtration enhancer. This is for vugs/large fractures.

7. NOMENCLATURE AND ACRONYMS

Abbreviations and Acronyms

Symbol	Description	Units
BHA	Bottom Hole Assembly	--
$CaCO_3$	Calcium Carbonate	--
CO_2	Carbon Dioxide	--
DEASP	Diatomaceous Earth/Amorphous Silica Powder	--
ECD	Equivalent Circulation Density	ppg
EIA	U.S. Energy Information Administration	--
GPM	Flow rate in gallons per minute	gpm
H_2S	Hydrogen Sulfide	--
HDR	Hot Dry Rock	--
HT	High temperature	--
HPHT	High Pressure High Temperature	--
KOH	Potassium Hydroxide	--
LCM	Lost circulation material	--
MD	Measured Depth	Ft
Micro-C	Micronized Cellulose	--
MW	Mud Weigth	ppg
NaOH	Caustic Soda	--
NPT	Non-Productive Time	--

O&G	Oil and Gas	--
P	Pressure	psi
ppb	Pounds per Barrel	ppb
ppg	Pounds per Gallon	ppg
PPT	Permeability Plugging Tester	--
PSD	Particle Size Distribution	--
PV	Plastic Viscosity	Cp
ROP	Rate of Penetration	ft/hr
SSMA	Sodium Salt Of Maleic Anhydride Copolymer	
T	Temperature	°F or °C
TVD	True Vertical Depth	Ft
WBM	Water-based mud	--
YP	Yield point	lbf/100ft^2

REFERENCES

Abrams, A., 1977. Mud Design To Minimize Rock Impairment Due To Particle Invasion. J. Pet. Technol. 29, 586–592. https://doi.org/10.2118/5713-PA

Alberty, M.W., McLean, M.R., 2004. A physical model for stress cages, in: SPE Annual Technical Conference and Exhibition. Houston, Texas, pp. 2867–2874. https://doi.org/10.2523/90493-ms

Alsaba, M., Al Dushaishi, M.F., Nygaard, R., Nes, O.M., Saasen, A., 2017. Updated criterion to select particle size distribution of lost circulation materials for an effective fracture sealing. J. Pet. Sci. Eng. 149, 641–648. https://doi.org/10.1016/j.petrol.2016.10.027

Alsaba, M., Nygaard, R., Saasen, A., Nes, O.-M., 2014. Laboratory Evaluation of Sealing Wide Fractures Using Conventional Lost Circulation Materials, in: SPE Annual Technical Conference and Exhibition. Amsterdam, The Netherlands. https://doi.org/10.2118/170576-MS

Amani, M., Al-Jubouri, M., 2012. The Effect of High Pressures and High Temperatures on the Properties of Water Based Drilling Fluids. J. Energy Sci. Technol. 4, 27–33. https://doi.org/10.3968/j.est.1923847920120401.256

Bauer, S., Galbreath, D., Hamilton, J., Mansure, A., 2004. Comments on High Temperature Plugs : Progress Report on Polymers and Silicates, in: Geothermal Resources Council Transactions. Geothermal Resources Council Annual Meeting.

Bauer, S., Gronewald, P., Hamilton, J., LaPlant, D., Mansure, A., 2005. High-Temperature Plug Formation With Silicates, in: SPE International Symposium on Oilfield Chemistry. The Woodlands, Texas. https://doi.org/10.2118/92339-MS

Blankenship, D., 2016. Drilling Challenges in Geothermal Reservoirs, in: ARMA-AAPG-SED Heat Workshop.

Bolton, R.S., Hunt, T.M., King, T.R., Thompson, G.E.K., 2009. Dramatic incidents during drilling at Wairakei Geothermal Field, New Zealand. Geothermics 38, 40–47. https://doi.org/https://doi.org/10.1016/j.geothermics.2008.12.002

Brown, D.W., 2009. Hot dry rock geothermal energy: important lessons from Fenton Hill, in: Thirty-Fourth Workshop on Geothermal Reservoir Engineering, Stanford University, Stanford. Stanford, California, pp. 9–11.

Caenn, R., Darley, H.C.H., Gray, G.R., 2016. Composition and properties of drilling and completion fluids, Seventh Ed. ed. Gulf professional publishing, Cambridge, MA, United States.

Cole, P., Young, K., Doke, C., Duncan, N., Eustes, B., 2017. Geothermal drilling: a baseline study of nonproductive time related to lost circulation, in: Proceedings of the 42nd Workshop on Geothermal Reservoir Engineering, Stanford, CA, USA. Stanford, CA, USA, pp. 13–15.

Cromling, J., 1973. Geothermal Drilling in California. J. Pet. Technol. 25, 1033–1038. https://doi.org/10.2118/4177-PA

Culver, G., 1998. Drilling and well construction, in: Geothermal Direct Use Engineering and Design Guidebook. Geo-Heat Center, Klamath Falls, OR, United States.

Dupriest, F.E., 2005. Fracture Closure Stress (FCS) and Lost Returns Practices, in: SPE/IADC Drilling Conference. Amsterdam, Netherlands. https://doi.org/10.2118/92192-MS

Finger, J., Blankenship, D., 2010. Handbook of best practices for geothermal drilling. Sandia Natl.

Lab.

Galindo, K.A., Zha, W., Zhou, H., Deville, J.P., 2015. High Temperature, High Performance Water-Based Drilling Fluid for Extreme High Temperature Wells, in: SPE International Symposium on Oilfield Chemistry. The Woodlands, Texas. https://doi.org/10.2118/173773-MS

Goodman, M.A., 1981. Lost circulation in geothermal wells: survey and evaluation of industry experience. United States. https://doi.org/10.2172/6238840

Grose, L.T., 1971. Geothermal energy: Geology, exploration, and developments. Part I. Color. Sch. Mines, Miner. Ind. Bull.

Hands Velsen, N., Kowbel Assen, K., Maikranz, S., Nouris Velsen, R., 1998. Drill-in fluid reduces formation damage, increases production rates. Oil Gas J. 96.

Hinkebein, T.E., Behr, V.L., Wilde, S.L., 1983. Static slot testing of conventional lost circulation materials. United States. https://doi.org/10.2172/6471455

Howard, G.C., Scott Jr., P.P., 1951. An Analysis and the Control of Lost Circulation. J. Pet. Technol. 3, 171−182. https://doi.org/10.2118/951171-G

Huy, P.Q., Sasaki, K., Sugai, Y., Ichikawa, S., 2010. Carbon dioxide gas permeability of coal core samples and estimation of fracture aperture width. Int. J. Coal Geol. 83, 1−10. https://doi.org/10.1016/j.coal.2010.03.002

Hyodo, M., Kitao, K., Furukawa, T., 2000. Development of Database System for Lost Circulation and Analysis of the Data, in: World Geothermal Congress 2000. Kyushu - Tohoku, Japan.

Jeennakorn, M., 2017. The effect of testing conditions on lost circulation materials' performance in

simulated fractures. Missouri University of Science and Technology.

Kaspereit, D., Mann, M., Sanyal, S., Rickard, B., Osborn, W., Hulen, J., 2016. Updated conceptual model and reserve estimate for the Salton Sea geothermal field, Imperial Valley, California, in: Geothermal Resources Council Transactions. pp. 57–66.

Lavrov, A., 2016. Lost circulation: Mechanisms and solutions, Lost Circulation: Mechanisms and Solutions. Elsevier Inc. https://doi.org/10.1016/C2015-0-00926-1

Liles, K.J., Sadler, L.Y., Goode, A.H., 1976. Geothermal Well Drilling Fluid Technology: A Literature Survey. | National Technical Reports Library - NTIS.

Magzoub, M.I., Salehi, S., Hussein, I.A., Nasser, M.S., 2020. Loss circulation in drilling and well construction: The significance of applications of crosslinked polymers in wellbore strengthening: A review. J. Pet. Sci. Eng. 185. https://doi.org/10.1016/j.petrol.2019.106653

Mansour, A., Dahi Taleghani, A., Salehi, S., Li, G., Ezeakacha, C., 2019. Smart lost circulation materials for productive zones. J. Pet. Explor. Prod. Technol. 9, 281–296. https://doi.org/10.1007/s13202-018-0458-z

Mansure, A.J., Bauer, S.J., Galbreath, D., 2004. Polymer Grouts for Plugging Lost Circulation in Geothermal Wells. Albuquerque, New Mexico, USA.

Marbun, B., Aristya, R., Pinem, H.R., Ramli, S.B., Gadi, B.K., 2013. Evaluation of Non Productive Time of Geothermal Drilling Operations – Case Study in Indonesia, in: Thirty-Eighth Workshop on Geothermal Reservoir Engineering Stanford University, Stanford, California, February 11-13. Stanford, CA, USA, p. 8.

Morita, N., Fuh, G.F., Black, A.D., 1996. Borehole breakdown pressure with drilling fluids - II. Semi-analytical solution to predict borehole breakdown pressure. Int. J. Rock Mech. Min. Sci. Geomech. 33, 53–69. https://doi.org/10.1016/0148-9062(95)00029-1

Nuckols, E.B., Miles, D., Laney, R., Polk, G., Friddle, H., Simpson, G., 1981. Drilling fluids and lost circulation in hot dry rock geothermal wells at Fenton Hill (Conference) | OSTI.GOV, in: Nternational Geothermal Drilling and Completions Technology Conference. Albuquerque, NM, USA.

Pálsson, B., Hólmgeirsson, S., Guomundsson, Á., Bóasson, H.Á., Ingason, K., Sverrisson, H., Thórhallsson, S., 2014. Drilling of the well IDDP-1. Geothermics 49, 23–30. https://doi.org/10.1016/j.geothermics.2013.08.010

Ran, Q., Wang, Y., Sun, Y., Yan, L., Tong, M., 2014. Identification and Prediction of Fractures in Volcanic Reservoirs, in: Gulf Professional Publishing (Ed.), Volcanic Gas Reservoir Characterization. Elsevier, pp. 203–271. https://doi.org/10.1016/b978-0-12-417131-2.00006-5

Refunjol, X.E., Marfurt, K.J., Le Calvez, J.H., 2011. Inversion and attribute-assisted hydraulically induced microseismic fracture characterization in the North Texas Barnett Shale. Lead. Edge 30, 292–299. https://doi.org/10.1190/1.3567260

Rickard, B., Samuel, A., Lee, C., Spielman, P., Cuadros, I., Long, J., Robert, E., Resource Group, G., Drilling Associates, A., Hughes Inc, B., 2012. KS 14 PUNA Geothermal Venture: Flawless Execution of Aerated Mud Drilling with Mud Motor in Hostile Environment, in: Hawai'i Institute of Geophysics & Planetology (HIGP) (Ed.), . African Rift Geothermal Conference.

Rossi, E., Jamali, S., Wittig, V., Saar, M.O., Rudolf von Rohr, P., 2020. A combined thermo-

mechanical drilling technology for deep geothermal and hard rock reservoirs. Geothermics 85, 101771. https://doi.org/10.1016/j.geothermics.2019.101771

Rüger, A., Tsvankin, I., 1997. Using AVO for fracture detection: Analytic basis and practical solutions. Lead. Edge (Tulsa, OK) 16, 1429. https://doi.org/10.1190/1.1437466

Salehi, S., Nygaard, R., 2011. Evaluation of new drilling approach for widening operational window: Implications for wellbore strengthening, in: SPE Production and Operations Symposium, Proceedings. Society of Petroleum Engineers (SPE), Oklahoma City, Oklahoma, USA. https://doi.org/10.2118/140753-ms

Samuel, A., Rickard, B., Spielman, P., Nickels, D., Otto, M., Pahler, M., Phillips, R., Guidry, C., 2011. Integrated Services Achieves Multi-String Casing Exit and Re-Drill in Geothermal Well: Kapoho State-11RD (Geothermal Well).

Sanyal, S.K., Enedy, S.L., 2011. Fifty Years of Power Generation at The Geysers Geothermal Field, California-The Lessons Learned, in: PROCEEDINGS, Thirty-Sixth Workshop on Geothermal Reservoir Engineering. Stanford, CA, USA.

Smith, P.S., Browne, S. V., Heinz, T.J., Wise, W. V., 1996. Drilling fluid design to prevent formation damage in high permeability quartz arenite sandstones, in: SPE Annual Technical Conference and Exhibition. Society of Petroleum Engineers. https://doi.org/10.2118/36430-ms

Taylor, J., 1997. Introduction to Error Analysis, the Study of Uncertainties in Physical Measurements, 2nd Edition, Second edition. ed, ieas. Published by University Science Books, 648 Broadway, Suite 902, New York, NY 10012, 1997.

Tuttle, J.D., 2005. Drilling fluids for the geothermal industry - Recent innovations, in: Transactions - Geothermal Resources Council. pp. 535–540.

Tuttle, J.D., Listi, R., 2003. A New Geothermal Drilling Fluid: Providing Temperature Stability, Inhibition, and Cost-Effectiveness for Worldwide Applications, in: Journal Geothermal Resources Council Transactions. Morelia, Mexico, pp. 47–50.

Van Oort, E., Friedheim, J., Pierce, T., Lee, J., 2011. Avoiding losses in depleted and weak zones by constantly strengthening wellbores. SPE Drill. Complet. 26, 519–530. https://doi.org/10.2118/125093-PA

Varnado, S.G., Stoller, H.M., 1978. Geothermal drilling and completion technology development. Albuquerque, NM, USA.

Vickers, S., Cowie, M., Jones, T., Twynam, A.J., 2006. A new methodology that surpasses current bridging theories to efficiently seal a varied pore throat distribution as found in natural reservoir formations. Wiertnictwo, Naft. Gaz 23, 501–515.

Visser, C.F., Eustes, A.W., Baker, W., Tucker, J., Quick, R., Nagle, T., Bell, J., Bell, S., Bolton, D., Nagandran, U., 2018. Geothermal Drilling and Completions: Petroleum Practices Technology Transfer.

Vivas, C., Salehi, S., Tuttle, J.D., Rickard, B., 2020. Challenges and Opportunities of Geothermal Drilling for Renewable Energy Generation. Geotherm. Resour. Counc. Trans. 44, 904–918.

White, D.E., Thompson, G.A., Sandberg, C.H., 1964. Rocks, Structure, and Geologic History of Steamboat Springs Thermal Area, Washoe County Nevada. Washington, DC, USA.

White, R.J., 1956. Lost-circulation Materials and their Evaluation., in: Drilling and Production Practice. American Petroleum Institute, New York, NY, USA.

Whitfill, D., 2008. Lost circulation material selection, particle size distribution and fracture modeling with fracture simulation software, in: IADC/SPE Asia Pacific Drilling Technology Conference 2008 - "Drilling Technology to Access Future Energy Demand and Environmental Challenges." Society of Petroleum Engineers, Jakarta, Indonesia. https://doi.org/10.2118/115039-ms

Zilch, H.E., Otto, M.J., Pye, D.S., 1991. The Evolution of Geothermal Drilling Fluid in the Imperial Valley, in: SPE Western Regional Meeting. Society of Petroleum Engineers (SPE), Long Beach, CA, USA. https://doi.org/10.2118/21786-ms